

THESIS

STREAMFLOW FORECASTING IN A SNOW-DOMINATED RIVER OF CHILE

Submitted by

Felipe Andrés Pérez Peredo

Department of Ecosystem Science and Sustainability

In partial fulfillment of the requirements

For the Degree of Master of Science

Colorado State University

Fort Collins, Colorado

Fall 2021

Master's Committee:

Advisor: Steven Fassnacht

Jason Sibold

Dave Barnard

ABSTRACT

STREAMFLOW FORECASTING IN A SNOW-DOMINATED RIVER OF CHILE

The combination of 10 years of drought in the Chilean Andes and an increased demand water supply and agricultural activities has created the need for better forecasts to inform water management and decision making. The existing water supply forecasts have been insufficient for the snow-dominated systems originating in the mountains, especially under the new drought conditions. Future climate change and inter-annual variability will further require the use of more detailed snowpack information to create better water supply forecasts.

This research focuses on the monthly water supply forecast for the basin upstream the flow gauging station called Río Aconcagua en Chacabuquito, in central Chile. This basin is located in the Mediterranean climate zone, originating at the highest peak in the Andes, Aconcagua. Meteorological data are collected at several stations in the lower elevations, and snowpack information, specifically monthly snow water equivalent (SWE) has been collected at the higher elevation Portillo snow course since 1951.

Here, a new methodology is created to improve the seasonal volume and the monthly distribution streamflow forecasts, using available information from operational and more representative stations. Results are being evaluated for the current snowmelt period (September 2020 to March 2021), with monthly updates. Improvements have been seen in the seasonal volume, due the use of historical data and because the new methodology also incorporates the

recent dry years, unlike the previous forecast model. Improvement in the monthly distributions are seen due the newly adopted methodology distribution.

DEDICATION

This work is dedicated to my wife Cynthia, to my parents, Flor and Humberto, and to the rest of my family. Also, I would like to dedicate this work to the people who through the years help me in my development as a person and as a professional. To my friends, and to my colleagues, thanks for that patience and those moments.

I would like to give the thanks to Professor Steven Fassnacht, for gave me the chance of work with him and to show and apply my abilities in this work. His help it was fundamental to reach the goal and to finish the task. His dedication, discipline and constancy were the headlights in my studies.

Thanks to the Ministry of Public Works' officials, who teach me and training me to be a better professional. Thanks for say those comments and to teach me that special way to watch the hydrology.

I would like to give thanks to my professor Roberto Pizarro. Thanks for those inspirational words and for let me in into this world.

Finally, this work is dedicated to the Chilean working-class people. Their hands and sweat are now presents in science.

TABLE OF CONTENTS

ABSTRACT.....	ii
DEDICATION.....	iii
LIST OF TABLES.....	vii
LIST OF FIGURES.....	x
FRONTISPIECE	1
1 INTRODUCTION AND OBJECTIVES	2
2 BACKGROUND.....	7
2.1 HYDROLOGICAL MODELLING.....	7
2.2 HYDROLOGICAL VARIABLES.....	9
2.3 WATER MANAGEMENT.....	10
2.4 MODEL IN USE.....	11
3 STUDY AREA AND DATA.....	14
4 DROUGHT ANALYSIS.....	21
5 METHODOLOGY.....	23
5.1 MODEL SET.....	23
5.1.1 VOLUME ESTIMATION.....	24
5.1.2 MONTHLY STREAMFLOW DISTRIBUTION.....	25

5.1.3 RISING LIMB-PEAK FLOW.....	27
5.1.4 RECESSION LIMB.....	29
6 RESULTS.....	32
6.1 MODEL IN USE VERSUS VOLUME OBSERVED.....	32
6.2 RESULTS DROUGHT ANALYSIS.....	34
6.3 CORRELATIONS.....	37
6.4 RESULTS VOLUME ESTIMATION.....	41
6.5 RESULTS RISING LIMB AND PEAK FLOW.....	42
6.6 RESULTS RECESSION LIMB.....	43
6.7 RESULTS FIRST APPROACH AND CORRECTION.....	44
7 DISCUSSION.....	47
7.1 DISCUSSION MODEL IN USE VS OBSERVED VOLUME.....	47
7.2 DISCUSSION DROUGHT ANALYSIS.....	48
7.3 DISCUSSION VOLUME ESTIMATION.....	49
7.4 DISCUSSION RESULTS RISING LIMB AND PEAK FLOW.....	49
7.5 DISCUSSION RESULTS RECESSION LIMB.....	50
7.6 DISCUSSION SET MODEL AND CORRECTION.....	50
8 CONCLUSIONS.....	52

9 FUTURE WORK AND RECOMMENDATIONS.....53

10 REFERENCES.....54

APPENDIX A: Information about the Portillo Snowcourse.....65

APPENDIX B: Data used.....68

LIST OF TABLES

Table 1: Summary information for the five stations used in the new forecast model, including the station BNA code (BNA is Banco Nacional de Aguas/Water National Bank), the variable(s) measured, the station elevation and the start of measurements.....	17
Table 2: Years of statistic used to calibrate (green) and to test (blue) the model, regarding the dependent variable to forecast.	17
Table 3: Mann-Kendall results. N= 55, Years from 1965 to 2020, p=0.05.	35
Table 4: Results Seasonal Volume.	42
Table 5: NSE. Results Seasonal Volume.....	42
Table 6: Parameters Rising limb and Peak Flow.....	42
Table 7: Average Monthly Temperatures.	43
Table 8: Results Rising Limb-Peak Flow.....	43
Table 9: NSE. Results Rising Limb-Peak Flow.	43
Table 10: Parameters Recession Limb.....	43
Table 11: Results Recession Limb.....	44
Table 12: NSE. Results Recession Limb.	44
Table 13: Results First Approach.	44
Table 14: Results. Correction Made with December Streamflow Controlled	44

Table 15: Results Volume.	45
Table 16: NSE. Results Volume.	45
Table 17: Observed Streamflow per month and per season, and the observed Volume per season (SUM VOL).....	45
Table 18: Data used. Volume Estimation.	68
Table 19: Data used. Monthly Streamflow (m ³ /s). Rising and falling limb.	69
Table 20: Data used. Monthly Temperatures (°C). Rising and falling limb.	70

LIST OF FIGURES

Figure 3-1: Site map showing a) the area upstream the flow gauge station Río Aconcagua en Chacabuquito (green). Into the image it can be observe the city of Los Andes and the river system upstream the station, the watershed location in Chile, and c) the stations used in this work, across the riverbed and at different elevations [image source: Google Earth].	16
Figure 3-2: The hydro-climatic normals (1981-2010) for a) the mean monthly hydrograph at the Aconcagua en Chacabuquito station, b) the distribution of precipitation at the three stations, and c) the mean monthly temperature at the Vilcuya station.	18
Figure 3-3: Approximate annual peak SWE for the period of record from 1951 through 2020. Measurements are usually taken in late August or early September depending on access to the site.	19
Figure 5-1: Scheme for the model. The results obtained in every section is used for the model deploy. The final volume is a sum of streams.	24
Figure 5-2: The box plot shows the historical range for the average monthly temperature from August to December.	28
Figure 5-3: The hydrograph between January and March, was elevated to a value bigger than December (Qd), which allow to get linear regression from December value, allowing the re-evaluation from this month when the real data is obtained.	30
Figure 6-1: Time series of the Volume Observed and the Volume estimated using the model in use. 1990 to 2020.	33

Figure 6-2: Correlation between time series of the Volume Observed and the Volume estimated using the model in use. 1990 to 2020.....33

Figure 6-3: The figure shows the SPI for 12 months (blue line), between 1971-2020 for the rain station Vilcuya. The year 2019 have the lowest register of rain in the last 50 years.....34

Figure 6-4: SPI for 12 months (blue line), between 2019-2020 for the rain station Vilcuya.35

Figure 6-5: The figure shows the exceedance probability for the variables. The values in the last ten years are clearly low (orange points).....36

Figure 6-6: Correlation between SWE and Seasonal Volume. The graph shows some data outsiders in transitions periods. The correlation has a R^2 of 0.61.....38

Figure 6-7: Correlation between Rain and Seasonal Volume. The correlation has a R^2 of 0.76.....38

Figure 6-8: The plot shows the correlation between the August runoff and Seasonal runoff. Looks a strong relationship, with problems in the high part, problems which can be improve with the rain and SWE as inputs as well in the analysis. The correlation has a R^2 of 0.85.....39

Figure 6-9: The graph shows the Start Month versus September, October, November, and December. The correlation is acceptable for each one, especially for November and December.....40

Figure 6-10: The plot shows the correlation between the December streamflow and the rest of months. The values are acceptable and use this month to forecast seems logical.....40

Figure 7-1 Monthly streamflow in the season 2010-2011 (driest in 30 years) versus the average streamflow.51

Figure 9-0-1: The figure shows the streamflow for each month in 2019, to the real values and to the forecast made by the DGA.66

Figure 9-0-2: The figure shows the streamflow for each month in 2016, to the real values and to the forecast made by the DGA.67

Figure A-1: The snow course (blue point), have its location because availability and logistic are required for these installations. Also, because it was built in 1951, so the resources and transport were limited. From left to right, north to south. Source: Google Earth.....65

Figure A-2: This picture shows the snow course and its posts. The equipment installed. The conditions of the snow course. From left to right, north to south. Photo from the author Felipe Pérez Peredo.....66

FRONTISPIECE

We are the dreams of our ancestors...

Elisa Loncón Antileo

1 INTRODUCTION AND OBJECTIVES

The climate of South America and particularly most of the Chilean territory is dominated by westerly air flows and the sea surface temperatures that determine modes of variation, including Oceanic Nino Index (ONI) and Pacific Decadal Oscillation (PDO) (Aravena, 2008). The Andes are the most important mountain range in the Southern Hemisphere, running near to the west coast of South America continuously from Colombia to the southern tip of the continent (Garreud, 2009). Countries as Perú, Bolivia, Chile, and Argentina are all dependent on snow and/or glacier melt for water supply (Bradley *et al.*, 2006; Peduzzi *et al.*, 2010; Masiokas *et al.*, 2013; Rabatel *et al.*, 2013; Saavedra *et al.*, 2016). Chile is extended for over 4000 km (17.5° to 56°S) along the Southern Andes, and much of the country is mountainous. The elevation of the Andes Cordillera decreases south-wards from peaks more than 6000 m.a.s.l. in the north of Chile (17.5° to 36°S) to mountains affected by fjords and channels in the south and austral (36 to 56°S) (Barcaza *et al.*, 2017). The summers in central territory are dry, while during the winter the westerlies can reach this region and generate frontal and orographic precipitation (Bown, 2008; Rutlant *et al.*, 1991).

Studies across different climate zones found an estimate of 32 percent of global discharge has a mountain contribution (Meybeck *et al.*, 2004; Viviroli *et al.*, 2007). In Chile, the mountains are the major source of water for the country, where much of the precipitation falls as snow. For this reason, the snowpack provides a large reservoir of water in snow-dominated river basin (Saavedra *et al.*, 2016). Even more, much of the Chile's population lives in the

lowlands below the mountains, in areas with arid and semiarid climates, where the annual water availability is less than 1000 m³/per capita (Valdes-Pineda *et al.*, 2014). This availability can be affected in the future by increases in the temperatures and decreases in precipitation, especially snow, which falls in mountainous areas, where climate change is resulting in upward shifts in the freezing point isotherm, coinciding with an overall warming of the Andean troposphere (Francou *et al.*, 2003; Perez *et al.*, 2010).

The understanding of water resources and the elaboration of hydrological models to assess water resources, floods and drought risks, and the effects of man-made and climatic change in watersheds is difficult and with lower results when hydrological data are scarce or absent (Winsemius *et al.*, 2009). This is especially true in places with complex terrain, such as the Andes, that coincide with areas where snow processes are dominant (Fassnacht *et al.*, 2014). A time series of hydrometeorological data is the basic input for the development of hydrological models, while the output is typically streamflow and/or runoff volumes, depending on the target (Phoung *et al.*, 2019). While hydrological models require meteorological data, these data may be limited, with poor quality, and in some cases, no meteorological records even exist in the watershed in study (Arsenault *et al.*, 2013). For that reason, the development of a hydrometeorological monitoring network is employed to address a wide range of environmental and water resources problems and conditions (Mishra & Coulibaly, 2009). A network can provide monitoring of several variables representing different components of the hydrological cycle and is designed to address one or more objectives (WMO, 1994; Mishra & Coulibaly, 2009). For rain gauge stations, the World Meteorological Organization (WMO, 1994) recommends a density of 250 to 575 km² per station for mountainous and rolling terrain, but the WMO does not propose

a method to identify the ideal location for stations (Arsenault *et al.*, 2013). For snow, the recommended density per snow course is one per 2000 to 3000 km² for less homogenous regions or accidental areas, and one snow course per 5000 km² in homogenous areas (WMO, 1994). For streamflow, there are no specific criteria for selecting the location of streamflow gauge stations, which results in numerous problems, including regional imbalances and overlapping (Joo *et al.*, 2019). However, regarding the WMO (1994) recommendation is one streamflow gauge station per 1000 km² for mountainous areas. In general, a sufficient number of streamflow stations should be located along the main stems of large streams to permit interpolation of discharge between stations (WMO, 1994).

The General Directorate of Water in Chile (DGA) is the governmental organization responsible for studying water resources, collecting the hydrometric information, and preparing the snowmelt forecast for the spring season every year (Código de Aguas, 1981). Thus, the accuracy of the forecast generated from historical data collected in the national hydrometric network is a priority for the DGA and must consider the effects of global warming and climate change on the environmental ecosystems, a topic that is important for researchers and society as a whole (Valdes-Pineda *et al.*, 2014). From the end of 19th century to the end of the 20th century, temperatures in the central portion of Chile (28° to 36° S) have shown a statistically significant warming of about 2.8°C. (Carrasco *et al.*, 2005). Even more, since 2010, a persistent drought has affected that Zone, leading to a marked decrease in water storage in reservoirs, and an extended forest fire season (Boisier *et al.*, 2016). Due to this new scenario of water scarcity, the DGA now has the need to improve their techniques to generate more detailed snowmelt forecasts. Since this drought over the last decade has created economic hardships in Chile, a

more detailed monthly streamflow forecast model would consider the recent hydro-climatic conditions and new water demands and allow for improved water resources decision-making.

This work focuses on the Aconcagua Basin that is located between 32.3° and 33°S, as it supports a million residents and a water-intensive economy dominated by agriculture and mining (Valdes-Pineda *et al.*, 2014; Webb *et al.*, 2020). The climate of the basin has high intra and inter-annual variability (Webb *et al.*, 2020). The hydrometeorological network in the basin has at least 50 years of data and follows the WMO regulations detailed in the Guide to Hydrological Practices WMO-N°168 (WMO, 1994). For this basin, the DGA has a lumped model and forecasting process; these need to be improved to yield better estimates for current and future requirements, including a better approach for the recession period. The existing, proprietary model is based specifically on the correlation between precipitation and runoff but does not consider snow water equivalent (SWE) directly, as it assumes SWE is correlated to rainfall. While the amount of snow higher in the basin, stored as SWE, is correlated to the rainfall at lower elevations, it is proposed that SWE be included in any new model. Using only rainfall, measured at lower elevations than where SWE is measured, will be valid only if the rainfall that occurs in the spring does not impact snowmelt runoff (Benitez *et al.*, 1976).

The purpose of this thesis is to create an updated snowmelt forecast model for the Aconcagua Basin using all available historical data. The specific objectives are as follows:

1 – to investigate the nature of all measured variables (Temperature or T, Precipitation or P, SWE, and streamflow or Q). Specifically, a) use a frequency analysis to determine the return period for extremely dry years, such as 2019-2020, b) determine the trends in the data,

specifically the rates of change from the Theil-Sen slope, and the statistical significance using the Mann-Kendall test, and c) the statistical significance in the difference of the recent decade of drought to the entire time series using the Mann-Whitney-Wilcoxon test.

2 – to determinate the correlation between the dependent variable Q and the three independent variables T, P, and SWE.

3 – to build a new statistical model that a) will be calibrate and evaluate for historical time periods, and b) compared to the existing model.

2 BACKGROUND

An effective management of limited water supplies is one of the critical components to the sustainability of populations (Pagano *et al.*, 2004). Reliable estimation of the volume and timing of snowmelt runoff is critical for water supply and flood forecasting in snow-dominated watersheds (Follum *et al.*, 2019). The access and availability to freshwater resources is a defining challenge of the 21st century, with most of the global population already vulnerable to water scarcity in multiple regions (Oki & Kanae, 2006; Mekonen & Hoekstra, 2016; Webb *et al.*, 2020). The numerical models are often developed and employed by water managers to understand and forecast snowmelt runoff within basins, under many scenarios and conditions (Follum *et al.*, 2019), which allow to have a certain volume or streamflow for the spring or summer season. In Mediterranean environments, the hydrological processes are largely variable both in time and space due to the high variability of precipitation regime, topography, and soil conditions (Milella *et al.*, 2012; Moussa *et al.*, 2007). Also, in these climates the snow has an important role as water reservoirs, especially in lowlands where the balance between precipitation and evapotranspiration is generally negative, and where floods and droughts occur periodically (Garcia-Ruiz *et al.*, 2011; San Miguel-Valladolid *et al.*, 2017).

2.1 HYDROLOGICAL MODELLING

Models are the mere representation of reality, which makes them subject to uncertainty (Nearing and Gupta, 2018). This uncertainty comes from different sources including driving or input variables (meteorology), derived model parameters (land use, soils, etc.), model structure

(conceptualization), and measurement data used for training and testing the model (streamflow, nutrient concentrations or loads, etc.) (Tasdighi *et al.*, 2018). The hydrological modeling in mountainous areas is especially problematic due to the complex terrain and elevation; the mountains store reservoirs of snow that melts slowly as the spring season progresses, and this provides water for the valleys below (Church, 1933). Further, to consider and anticipate the impacts of climate change, especially warming, it is important to characterize the influence of the snowpack on streamflow timing and to identify future trends (Whitaker *et al.*, 2008; San Miguel-Vallelado *et al.*, 2017).

The output from hydrological modeling depends on the input data and often various parameters. Therefore, efficient and effective use of observed data is crucial for calibration of complex spatially distributed process-based models. There are numerous applications of automated calibration methods to minimize error; however, even with these techniques the results usually have some uncertainty (Ahamadi *et al.*, 2014). Accumulated error may seriously affect estimates for dry and/or wet conditions (Nash & Sutcliffe, 1970). Even for the commonly used power model ($\hat{y}=ax^b$), the computed correlation coefficient can be a poor estimation or goodness of fit due to model bias (McCuen *et al.*, 2006).

This work uses a Linear Regression Model since limited point information are available that are correlated. Such models are widely employed in the hydrological sciences as they provide a convenient framework for estimating or predicting the behavior of a certain variable. The use of regressions has found applications in regionalization studies because the main objective (streamflow-volume) can be derived from correlations with random hydrological variables (Naghettoni, 2017).

2.2 HYDROLOGICAL VARIABLES

The term “water tower” is used to describe the mountains as a source of water. The Chilean Andes are such a representation since they are a source of water for a big portion of the country, driven by snowmelt, which, in Chile, normally occurs between September and March. To understand the water availability, the snowmelt is modelled using statical regression with meteorological variables, which allows for forecasting of the seasonal volume and monthly runoff (Fassnacht *et al.*, 2014). The main variable is SWE (scientifically expressed in millimeters of water), which is manually or automatically measured, and a comprehensive understanding of the distribution of the seasonal mountain snowpack is important to improve hydrologic models used for forecasting water availability and distribution (Sexstone & Fassnacht, 2014). However, such distributed SWE data are often not available (Fassnacht *et al.*, 2003).

The snowpack has a central role in the water availability; however, the Surface Water Input (SWI), which is the combination of snowmelt and rain (Niemeyer *et al.*, 2016), also is important. The timing of SWI is highly sensitive to the phase of precipitation (rain or snow) because SWI timing is effectively synchronous with precipitation for rain events but is asynchronous for snow events by hours or even months depending on melting timing (Niemeyer *et al.*, 2016). Therefore, rainfall has an important role in the streamflow generation, and thus forecasting, particularly in the early in the melt season. An accurate estimate of precipitation inputs are required for effective hydrological modeling (Fassnacht *et al.*, 1999) in both applied and research settings, especially when snow storage delays the transfer of precipitation to surface runoff, infiltration, and generation of streamflow (Harpold *et al.*, 2016). Elevated streamflow generation due to winter rain is most likely in places with relatively warm and wet

winters, where subsurface storage is elevated throughout the cold season, as opposed to colder areas with persistent snowpacks where winter rain is less likely, and winter subsurface storage remains low (Hammond & Kampf, 2020).

The spatial distribution of near-surface air temperature (T_{ns}) over mountains is an important input to hydrological, glaciological, and ecological studies. The surface temperature depends on elevation as well as other physiographic features (terrain slope and exposition) and land cover, making estimation of the spatial distribution and temporal evolution difficult (Gonzalez & Garreaud, 2016; Collados-Lara et al., 2021).

The interaction between surface (atmospheric) and subsurface (stream bed, hyporheic exchange, and groundwater flow) processes determining the thermal characteristics of streams are complex. However, representing these processes in regions with limited data, and at a scale applicable to environmental management-related questions, presents a significant challenge (MacDonald *et al.*, 2014). The streamflow records, as part of the model, provide an advantage because streamflow provide an integrated record of the effects of changes in precipitation, snowmelt, temperature, and evapotranspiration across spatially extensive areas. Also, the streamflow records from alpine areas provide data from areas of rugged topography where meteorological instrumentation and data are often sparse (Reinsfield *et al.*, 2014).

2.3 WATER MANAGEMENT

Since the use of water is crucial for human existence, its management requires hydrological efficiency to guarantee economic and environmental sustainability. Thus, it is crucial to have appropriate public policies to ensure an efficient governance system, as well as

information on the availability of water resources in the country, especially where precipitation varies significant (Valdes-Pineda *et al.*, 2014). The situation is further complicated when long-term climate trends effect the sustainability of regional mountain water resources and therefore irrigated agricultural productivity, and to date, these are poorly constrained (Webb *et al.*, 2020). Streamflow data are used for important environmental decisions, such as specifying and regulating minimum flows, managing water supplies, and planning for floods hazards. Flow data guide to the operative management of reservoirs and dams, and thus affect economic returns (McMillan *et al.*, 2016), which is even more complicated when it is combined with the possible effects of global warming. This could include the increase in elevation of the zero degree isotherm, and/or snow line, within the Andes Mountains, thus reducing the water availability in the springtime and summertime (Valdes-Pineda *et al.*, 2014). Finally, the streamflow and water yield from mountainous areas are of direct economic and social importance to communities, states and nations downstream, and often form a primary focus for governments and water managers (Reinsfield *et al.*, 2014).

2.4 MODEL IN USE

The new model or method should improve the results for scarcity scenarios, and to use the online information for forecasting. Due the drought periods in the last time and the increasing demands, the requirements about the forecast for seasonal and monthly values has increased. The model in use it has intellectual restriction because its elements and structure were development under copyright restrictions, to avoid its use for non-governmental activities, for this reason only can be describe in general terms. The model in use, it does include hydrological correlation, but does not provide reasonable forecasting results in some seasons

and based in some climatic conditions, and thus it does not satisfy the needs of the Directorate. Examples of the current model are presented in section 5.1.

The model in use is producing good forecasts for certain periods, but it also relies on the expertise of the forecaster and what is need it, it is an automatic model, to produce the forecast and the streamflow distribution. The model in use is a lumped model because it has several parameters calibrated using non-recent information to forecast the streamflow in a watershed's junction. The model in use to consider SWE, rain and streamflow (August) as inputs, and forecasts the streamflow for each month in the station "Río Aconcagua en Chacabuquito", which finally is summed to provide the volume per season. In the last ten years the results have been quite varied and very depending on the forecaster's expertise and knowledge, which is a problem when the appropriate expert is not available or does not exist.

Another problem with the model in use is that the forecast cannot be updated it, change it, or re-evaluated it in the middle of the season, such as in December. Climatic conditions vary over a season and other forecast models are updates monthly (e.g. Pagano et al., 2004, although the U.S. Natural Resources Conservation Service forecasts are seasonal runoff volumes). While the existing model can produce reasonable estimates of the seasonal runoff volume, the individual monthly forecasts can poor. Since water management decisions are based on the streamflow forecasts, these differences can impact in the use and distribution of water, especially in a year with lowers water levels such as 2019. Further, providing accurate forecasts to determine the peak flow month can be difficult, especially in a wet season. These high flow forecasts can be very important the safety of water distribution and related infrastructure, as well as tourism and agricultural activities that use the same forecast information. The Figure 9-2,

Appendix, shows the problem forecasting the peak with the model in use, especially in a normal season as it was the 2016-2017, when the peak flow from it, it was very low regarding the Observed Value to December.

3 STUDY AREA AND DATA

The study basin is the upstream area of 2,400 km² at the flow gauge station called “Río Aconcagua en Chacabuquito” (Figure 3-1 and Table 3-1). The station is an important point of water distribution controlled by the DGA. Its information is an input for many users downstream the station, where mostly of agriculture activities are concentrated and represents the 7.6% of entire basin’s area (7333 km²) (Valdes-Pineda *et al.*, 2014; Webb *et al.*, 2020). The maximum streamflow occurs in the springtime, reaching a peak of about 80 m³/s, usually in December (Figure 3-2a). This basin is snowmelt dominated, with flows increasing in September or October and remaining higher through March. The influence over those months by other sources of water, as glaciers, in basins located in the central Chilean Andes are around 10-13% of the monthly average streamflow (Bravo *et al.*, 2016), been the area covered by ice in the Aconcagua’s basin about 121 km² (Bown *et al.*, 2008).

Four other stations are used in this research (Table 3-1). A period of about 50 years is used in this investigation to have a consistent time series and to include multiples hydrological scenarios (Table 3-2).

The basin has a Mediterranean climate with the mean annual station/measured precipitation varying from about 270 mm in the valley at Los Andes (825 m.a.s.l.) to about 510 mm at Riecillos (Figure 3-2b). The largest monthly precipitations in the wintertime from April through August (Figure 3-2b) and represents the season for the snowpack accumulation and

ripening. Only the station Vilcuya has a continuous temperature data from 1970 and shows cooler temperature in the winter with warming starting in August or September (Figure 3-2c).

The average peak SWE in the station Portillo (3033 m.a.s.l) are 595 millimeters per season, but there is much inter-annual variability over the period of record from 1951 to 2020 (Figure 3-3). A drought occurred in the late 1960s and since about 2010 (Figure 3-3). The Portillo snow course is located near to the Argentinian border (Figure 3-1), has a north facing aspect at the bottom of a valley (Figures A-1 and A-2). Sampling occurs at the end of the season, which typically is at the end of August or beginning of September, depending on the access and weather conditions in each season.

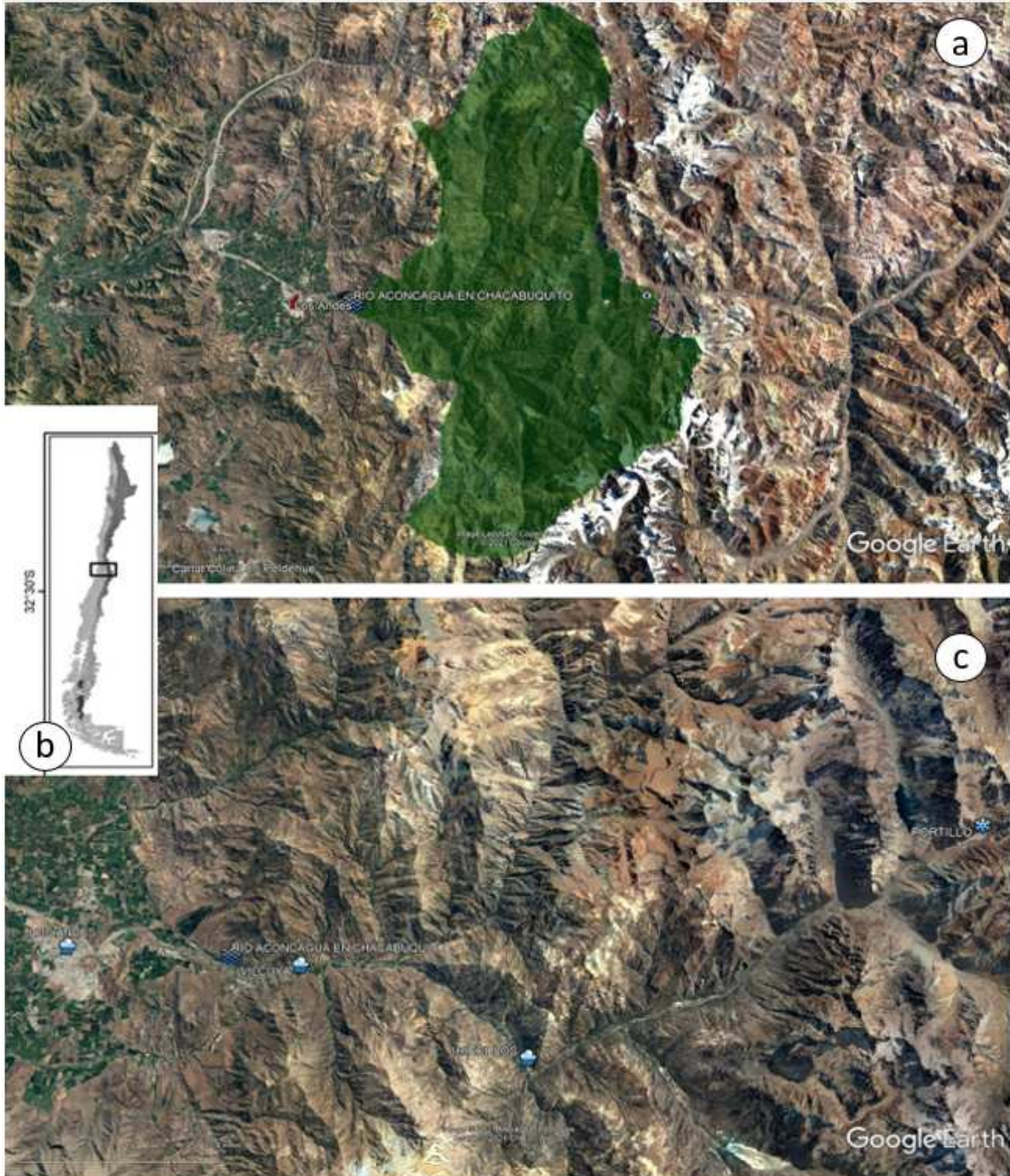


Figure 3-1: Site map showing a) the area upstream the flow gauge station Río Aconcagua en Chacabuquito (green). Into the image it can be observe the city of Los Andes and the river system upstream the station, the watershed location in Chile, and c) the stations used in this work, across the riverbed and at different elevations [image source: Google Earth].

Table 1: Summary information for the five stations used in the new forecast model, including the station BNA code (BNA is Banco Nacional de Aguas/Water National Bank), the variable(s) measured, the station elevation and the start of measurements.

Station Name	BNA code	Variable	elevation (m.a.s.l.)	Start Year
Los Andes	05410007-8	precipitation	825	1971
Vilcuya	05410006-k	precipitation /temperature	1060	1965
Riecillos	05403006-1	precipitation	1284	1930
Portillo	05401007-9	SWE	3033	1951
Río Aconcagua en Chacabuquito	05410002-7	streamflow	937	1936

These stations and its variables are the available information for the model construction and to forecast seasonal volume and streamflow across the season. The data have undergone quality control from the Chilean Government following the WMO standards for location and quality control processes (WMO, 1994). The information derived from a forecast model must give answers for a variety of possible climatic and thus hydrologic conditions since a big part of the Aconcagua Basin is dedicated to agricultural cultivation and energy. The Table 3-2 shows the years of statistic used to calibrated and to test the model, regarding the depended variable to estimated, streamflow or seasonal volume. For both variables, the testing period it has the same years.

Table 2: Years of statistic used to calibrate (green) and to test (blue) the model, regarding the dependent variable to forecast.

Dependent Variable											
Volume	Streamflow	Volume	Streamflow	Volume	Streamflow	Volume	Streamflow	Volume	Streamflow	Volume	Streamflow
1965		1975	1975	1986	1986	1996	1996	2006	2006	2016	2016
1966		1977	1977	1987	1987	1997	1997	2007	2007	2017	2017
1967		1978	1978	1988	1988	1998	1998	2008	2008	2018	2018
1968		1979	1979	1989	1989	1999	1999	2009	2009	2019	2019
1969		1980	1980	1990	1990	2000	2000	2010	2010	2020	2020
1970	1970	1981	1981	1991	1991	2001	2001	2011	2011		
1971	1971	1982	1982	1992	1992	2002	2002	2012	2012		
1972	1972	1983	1983	1993	1993	2003	2003	2013	2013		
1973	1973	1984	1984	1994	1994	2004	2004	2014	2014		
1974	1974	1985	1985	1995	1995	2005	2005	2015	2015		
Calibration	Testing										

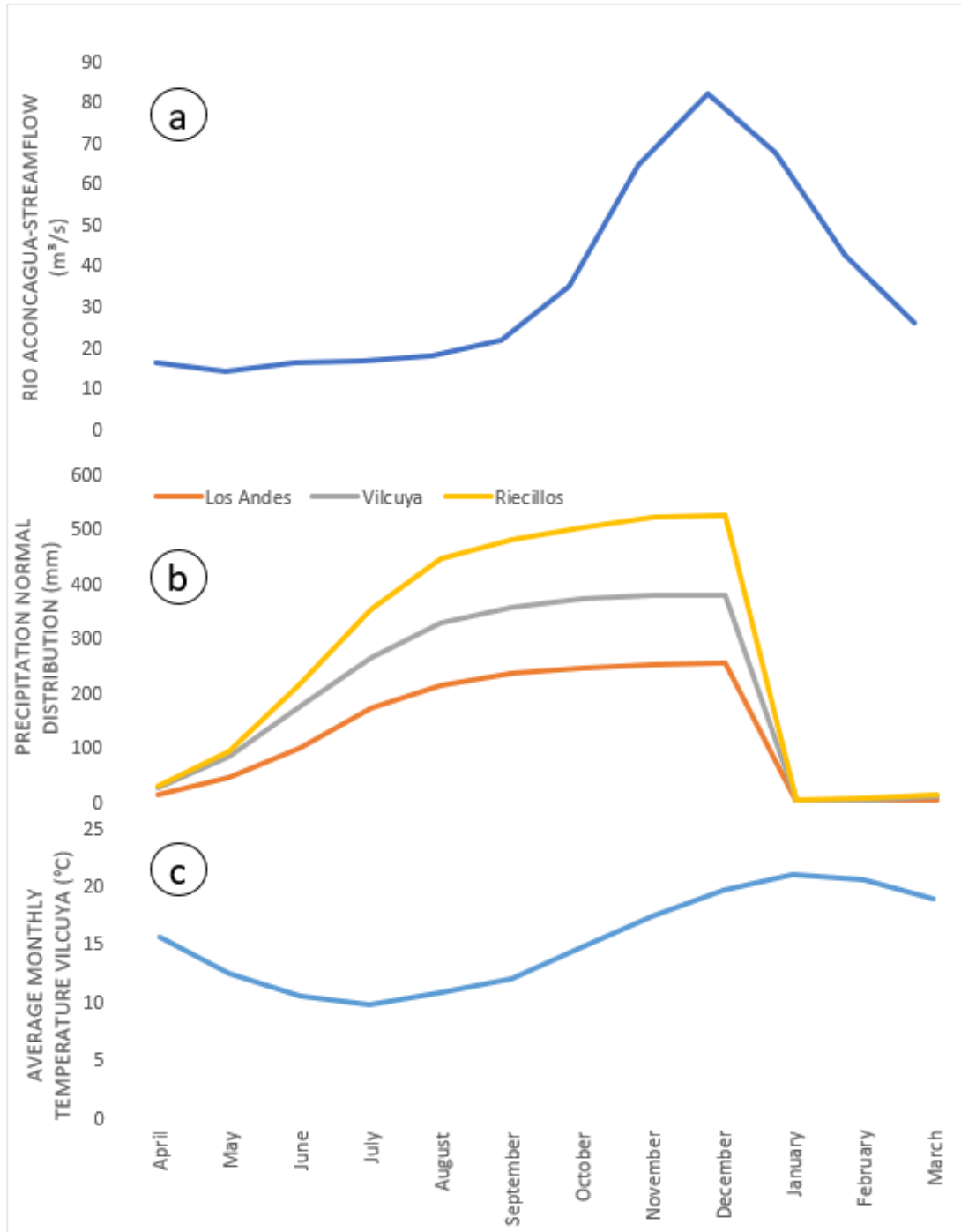


Figure 3-2: The hydro-climatic normals (1981-2010) for a) the mean monthly hydrograph at the Aconcagua en Chacabuquito station, b) the distribution of precipitation at the three stations, and c) the mean monthly temperature at the Vilcuya station.

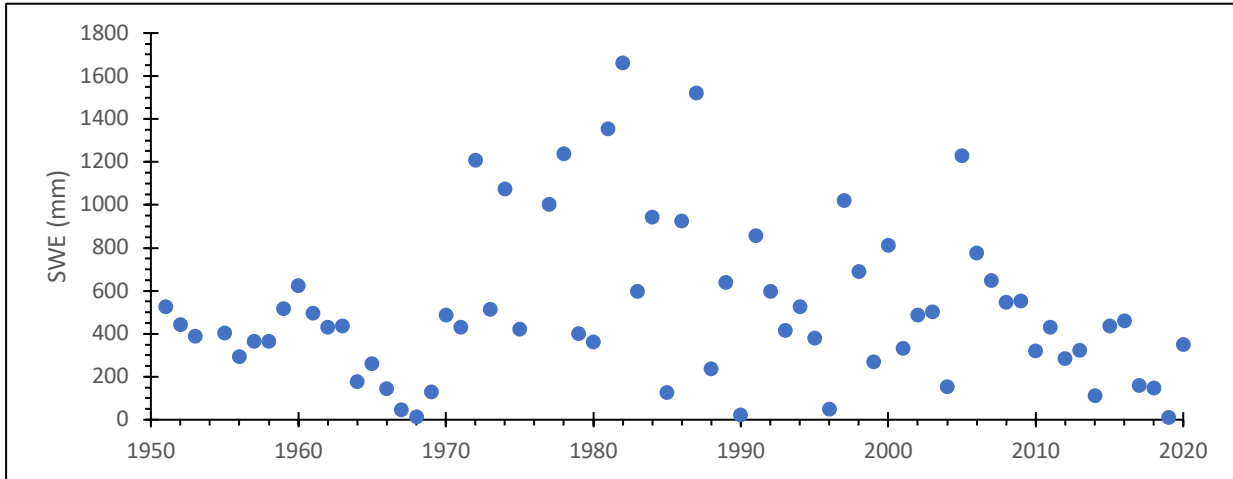


Figure 3-3:: Approximate annual peak SWE for the period of record from 1951 through 2020. Measurements are usually taken in late August or early September depending on access to the site.

Prior to 2019, the period between 2010-2015 was known as the Chilean megadrought (Boisier *et al.*, 2016; Garreaud *et al.*, 2017; Webb *et al.*, 2020). The last ten years from 2010 can be identified as drought (Figure 3-4b), and forecast accuracy was low during this period creating problems for water supply and distributions. This is especially true for the 2019 forecast when SWE was almost zero (Figure 3-4a). The historic dry period from 1968 to 1970 also created problems for water supply and distribution (Figure 3-4). These periods can be contrasted with peaks of precipitation, SWE and streamflow in the 1980s (Figure 3-4). The Figure 3-5 shows the range of years

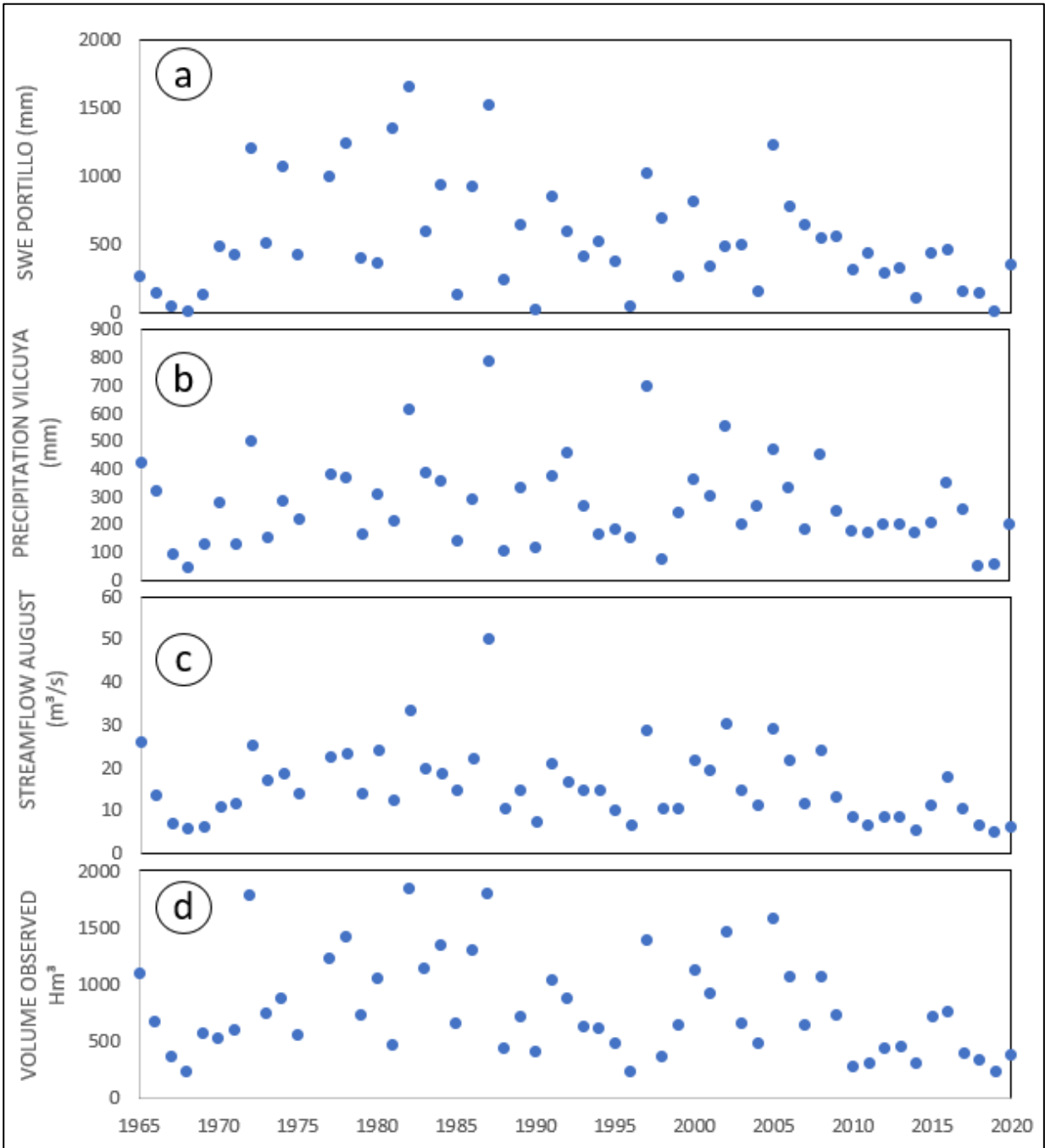


Figure 3-4: The hydro-climatic time series from 1965 to 2020 for a) SWE, b) precipitation at Vilcuya, c) August streamflow. and d) observed annual run off volume.

4 DROUGHT ANALYSIS

Since drought yields low values of runoff volumes, SWE, and precipitation, especially in the last 10 years, the nature of these drought years was statistically analyzed. The first analysis used to characterize the drought of this period was the Standard Precipitation Index (SPI) (McKee *et al.*, 1993; WMO, 2012), which is used by the General Directorate of Water to evaluate drought conditions.

The SPI calculation for any location is based on the long-term precipitation record for a desired period. This long-term record is fitted to a probability distribution, which is then transformed into a normal distribution, the period under the evaluation is contrasted against a threshold. A Positive value means a wet condition and an extreme negative value represents a dry condition. The SPI quantify deficits for multiple timescales, which reflect the impact of drought on the availability of different water resources (McKee *et al.*, 1993; WMO, 2012).

The second analysis is to evaluate changes or trends over time. The Theil-Sen slope (Gilbert, 1987) was used to estimate the rate of change for volume, SWE, precipitation and streamflow in August over the study period. The Mann-Kendall test (Gilbert, 1987) was used to compute the statistical significance level for the trends at the 0.05 confidence level. These widely used non-parametric tests characterize the tendencies of a variable throughout the years. The Mann-Kendall trend test is a function of the ranks of the observations rather than their actual values, and is not affected by the assumption of normally distributed making it less sensitive to outliers; thus it is suitable for hydrological analysis (Hamed, 2007).

The third assessment was to determine the exceedance probability of specific, extreme years compared to the entire time series. The value for each year of interest (X_t) was compared to the mean (\bar{X}) and standard deviation (σ_x) computed from the time series to determine the number of standard deviations (Z_t) that X_t was different than \bar{X} (Fassnacht *et al.*, 2004). Using the Gumbel Distribution, the return period was computed. This distribution was selected as it is widely used for extreme values or events in frequency analysis of hydrologic variables (Naghetini, 2017).

5 METHODOLOGY

A new forecast model must provide two components. The first part is the seasonal volume forecast, which is the total volume per season between September and March (spring and summer time). The second part is to determinate the volume or streamflow for each month from September to March. Initially, the correlations between the different variables were assessed. Once the seasonal volume and monthly distributions were estimated, a statistically analysis was performed on each formulation and regressions. Linear regressions will be used with a minimum correlation coefficient (R^2) of 0.6, which is considered satisfactory for longer time scales, i.e., monthly or seasonal (Erickson & Stefan, 1996; Mohseni & Stefan, 1999). Further, regression analysis has become a widespread used tool for data description, estimation, and forecasting in hydrology, due to the simplicity of its application framework and its theoretical basis (Naghetini, 2017).

5.1 MODEL SET

The model setting for a season is made using the values estimated in each section. For this reason, the volume estimated is used in the Rising Limb-Peak Flow section. The value of December (Q_d) from this section is used for the calculation of each month from January to March. Each percentage and volume (Hm^3) must be converted in m^3/s regarding the needs and forecasting presentation. The final seasonal volume it will be the sum ($\sum Q$) of each month. The purpose of the model is to represent the natural distribution of the streamflow across the season.



Figure 5-1: Scheme for the model. The results obtained in every section is used for the model deploy. The final volume is a sum of streams.

5.1.1 VOLUME ESTIMATION

The snowmelt forecast is based in the relationship precipitation-runoff, and between precipitation (rain-snow), SWE, annual runoff and snowmelt runoff, there's some interactions (Benitez *et al.*, 1970). Interactions which are going to be evaluate using data from 1965 to 2020 in all the variables but leaving apart some years to the testing.

The consideration of each variable as a water height, also makes easy and understandable the results due to changes in the variables. The final volume finally is a sum of water heights portions from precipitation, SWE and August runoff because it's assume that's volume value (mm), is a result and effect of the other water heights (mm) reserved, fallen, and circulating in the watershed.

With these conditions the seasonal volume (VOL. EST.) can be determinate as follow:

$$\text{VOL. EST. (mm)} = \text{PRECIPITATION PROPORTION (mm)} + \text{SWE PROPORTION (mm)} + \text{START MONTH PROPORTION (mm)}$$

The adjust of each parameter it will help to understand the importance of each station in the final expression. It will have two pools of data, one for calibration and other for testing. For

this reason, the proportions which is represented by a parameter of each station and variables would be evaluated as follow.

The precipitation will be evaluated using the information from three stations: Los Andes, Vilcuya and Riecillos. The use of one parameter for each station value is considered. The formula for precipitation proportion is next:

$$\text{PRECIPITATION PROPORTION (mm)} = \mathbf{a} * \text{Los Andes (mm)} + \mathbf{b} * \text{Vilcuya (mm)} + \mathbf{c} * \text{Riecillos (mm)}$$

where **a**, **b** and **c** are calibration parameters.

The SWE portion it will be evaluated as follow and using the information from the snow course Portillo, the next expression characterizes the SWE proportion:

$$\text{SWE PROPORTION (mm)} = \mathbf{d} * \text{SWE Portillo (mm)}$$

where **d** is a calibration parameter.

The August runoff or “Start Month” also have an important role in the seasonal volume as Figure 13 shows, particularly for dry season and average seasons. Showing important correlations for wet seasons. The next expression defines the “Start Month” proportion:

$$\text{START MONTH PROPORTION (mm)} = \mathbf{e} * \text{START MONTH (mm)}$$

where **e** is a calibration parameter.

5.1.2 MONTHLY STREAMFLOW DISTRIBUTION

Due the nature of the Aconcagua Basin, to be a snow-fed basin, the most important period of the year is the spring and summer time, when the volumes reached are clearly biggest and the average peak flow reached is of almost 80 m³/s in December, with a clear descend between

January and March, indicating the exhaustion in the watershed. These conditions and characteristic can indicate that a monthly streamflow is finally the resulting of some relationships between the seasonal volume, the temperatures in the season and the streamflow in August or -Start Month-. The monthly average hydrograph for the basin in the spring season and summer is showed in the Figure 3-2.

The temperature it was included in the model because particularly in high elevation basins, is one of the most sensitive inputs in estimating snowmelt-runoff (Martinec et al., 2008; Tahir et al., 2011; Kang & Lee, 2014). The effects of this variable over the monthly streamflow are going to be evaluated, also because the responses of water resources to temperature is important, considering futures scenarios and climate change (Woodhouse et al., 2016). Figure 3-2 shows the temperature from August until December, and the streamflow for same period. For this section, the data used is from 1970 to 2020, this to have equality in the information.

Streamflow in most snowmelt-dominated mountain systems follows a typical seasonal pattern: low flow in the fall and winter month, snowmelt surge in spring, peak flow in December, followed by a slow recession to base flow in March (Dunne & Leopold, 1978; Painter *et al.*, 2017). For this reason, a streamflow hydrograph from the station “Río Aconcagua en Chacabuquito” can be separated in two parts, a rising limb, which reflected the increases in discharge from an event, and a recession curve, which represent streamflow maintained at least in part by discharge from watershed storage (Thomas *et al.*, 2015). The peak flow is included in the rising limb. This differenced analysis implies the use of two pools of months in the work.

These relationships allow to determinate that an increase or decrease in the streamflow or volume measured in August or Start Month, affect the percentage in each month, but finally the temperature can play an important role into the snowmelt process. The next expression shows this relationship:

$$\text{Monthly Percentage} = \% \text{ Volume Month} + \% \text{Temp Month}$$

5.1.3 RISING LIMB-PEAK FLOW

This section of the hydrograph represents the peak expression for the streamflow and a big part of the season volume as well. This period goes between September and December, month on which the peak flow normally is reached. In this period, each month also typically represents a percentage of the seasonal volume. This percentage can vary regarding the watershed conditions and season temperatures. This relationship allows to determinate that an increase or decrease in the streamflow or volume measured in August or Start Month, affect the percentage in each month. The next expression shows this relationship:

$$\% \text{ Volume Month} = \alpha \frac{\text{Volume Start Month Season } i}{\text{Volume Season } i}$$

where α is a parameter to calibrate for each month.

Another component o part in the Monthly percentage, is the use of the temperature because the influence of this variable can incorporate the dynamics in the streamflow due the

season's temperatures, considering the monthly temperature from August as value of contrast. The Figure 5-1 shows the historical temperatures using box plots from August to December, on which is observed a variability regarding the season. The variation in each month is around 5°C.

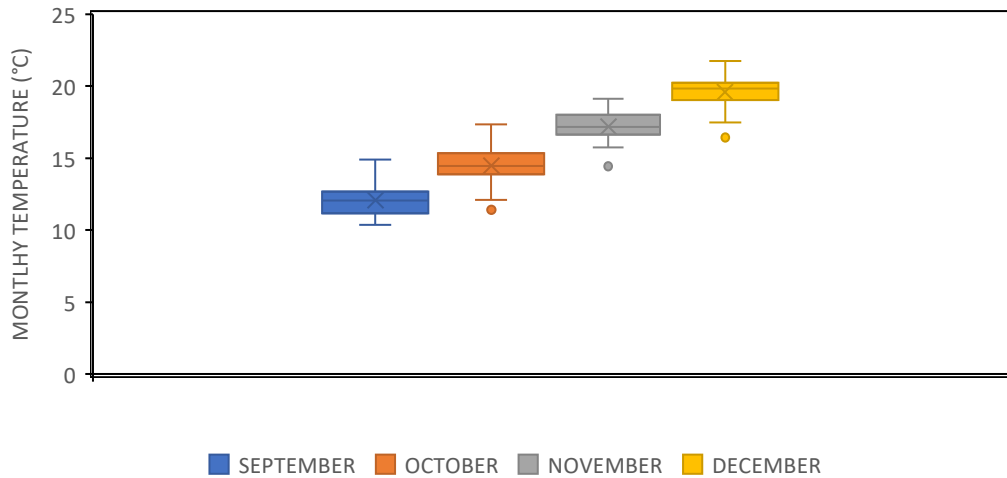


Figure 5-2: The box plot shows the historical range for the average monthly temperature from August to December.

The percentage for each month, also may have an influence due the monthly temperature, especially in a warm season, when the temperatures to accelerate the snowmelt processes altering the forecasting. For this reason, the use of the temperature registered in August or Start Month follows the logical of using this month as input to incorporate the watershed's conditions in the analysis. The contrast for the Start Month is the average monthly temperature for September until December. This proportion is showed in the next expression:

$$\%Temp\ Month = \beta \frac{\text{August Temperature Season } i}{\text{Monthly Average Temp Month}}$$

where β is a parameter to calibrate for each month.

The final percentage for each month is obtained summing the “% Volume Month” and the “%Temp month”, the next expression shows the term:

$$\text{Monthly Percentage} = \alpha \frac{\text{Volume Start Month Season } i}{\text{Volume Season } i} + \beta \frac{\text{August Temperature Season } i}{\text{Monthly Average Temp Month}}$$

α, β , parameters to be calibrate for each month.

The percentage for each month will provide the volume and the streamflow for the period between September and December.

5.1.4 RECESSON LIMB

This part of the hydrogram has a strongly correlation with the peak flow reached in December due the snowmelt. Also, between January and March, the of water availability begins a notorious decreasing, finishing in March with a streamflow lowers than 30 m³/s. This section is simple in its analysis because also represent the finals discharges for the season in the watershed due the exhaustion in the resource. Even more, each month have a strong correlation with December (Peak flow), and their behaviors are results of its magnitude and intensity with this month.

To improve and make easier the adjust with linear regression the hydrograph was transformed as next. The linearly detected between December and the months of the dry period, it cannot be use with decreasing numbers, but it can be fixed, raising the plot over those

points to have a positive increase from December, creating a new value called y' . The next Figure 5-2 shows the explained.

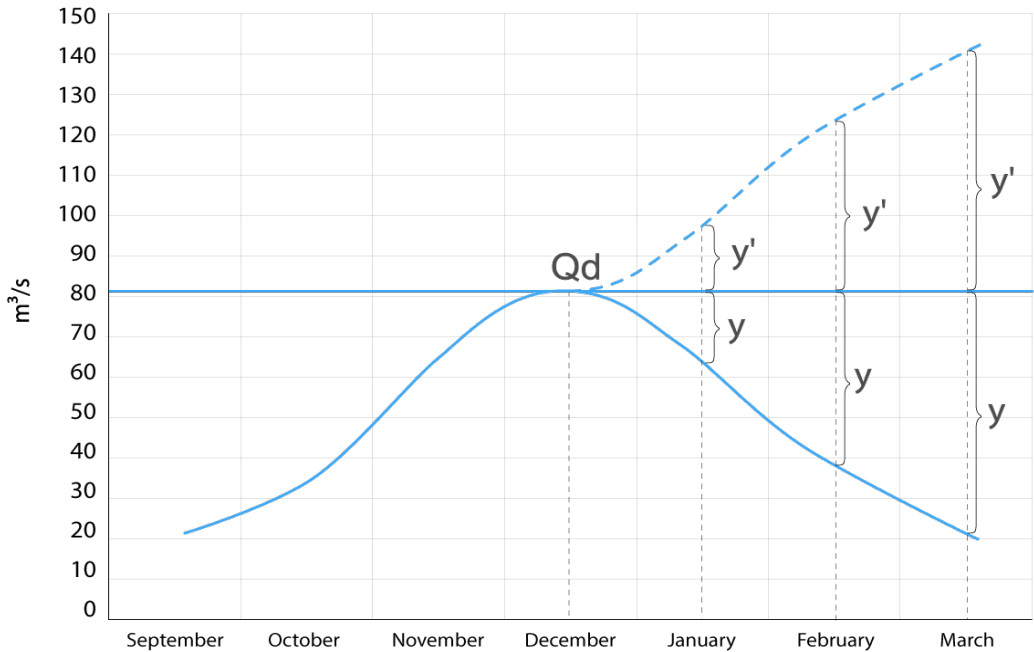


Figure 5-3: The hydrograph between January and March, was elevated to a value bigger than December (Qd), which allow to get linear regression from December value, allowing the re-evaluation from this month when the real data is obtained.

The new points (y') will be the value used for the linear regression, considering the months December as a base value and part of the equation. The next expressions explain how y' is calculated.

$$y' = 2y + Qd$$

The model recreates the value y' because it was the value used to calibrated it. The value for each y' is given by the next formula.

$$y' = \alpha Qd$$

α , parameter to be calibrate for each month.

However, to know the value of y , and through that, to know the value for January, February and Mach, the next expression is used:

$$y = \left(\frac{y' - Qd}{2} \right)$$

Once, the value of y is finally estimated, the monthly streamflow can be calculated with the next expression:

$$\text{Monthly Streamflow (x)} = Qd - y$$

Each month, between January and March have a unique equation for the estimation of y' , using in the calculation the value estimated in December in the Rising Limb-Peak Flow section. This also allow, when the streamflow is controlled in December, re-evaluated the streamflow forecast for the rest of the season.

6 RESULTS

The results estimated in each section were the values for the years 2011, 2012, 2013, 2014, 2016, 2017 and 2020. These years were used in the testing period to evaluate the model and methods. The years selected also represent one the driest period registered in the flow gauge station Río Aconcagua en Chacabuquito. However, to evaluate the results against the model in use, a comparison between the model in use versus the volume observed was made and is showed at next. Also, to make clearer and more understandable the dry condition suffer by the watershed in the last time, a drought analysis is presented at next.

6.1 MODEL IN USE VERSUS VOLUME OBSERVED

The results expected from the new method should be better that the results from the model in use. The next figure shows the results for the volume from the model in use and the Observed Volume per season from 1990. The differences between both, observed and estimated, seems to be something often since 2010, year when start the drought period.

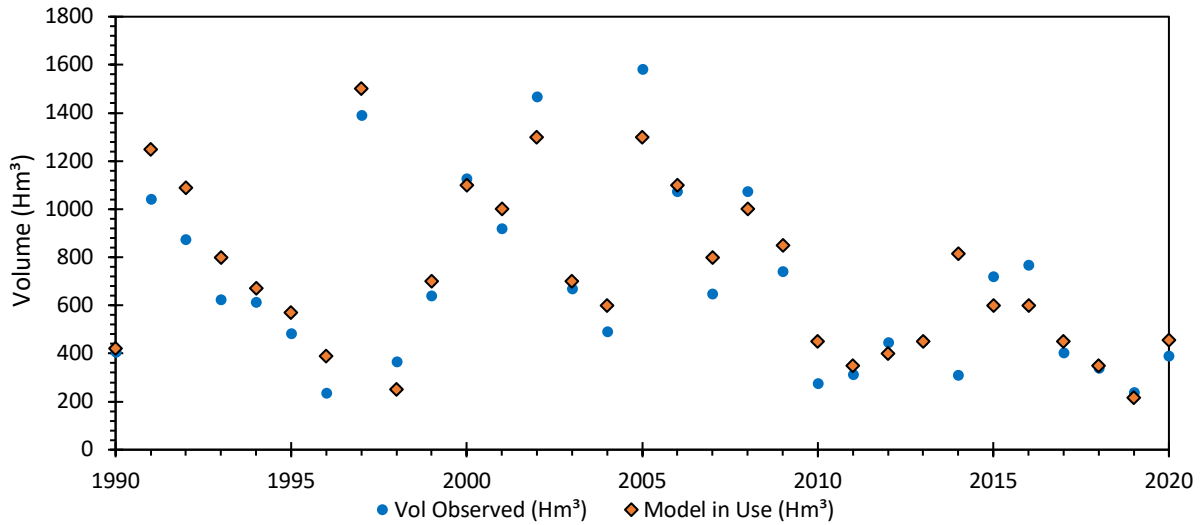


Figure 6-1: Time series of the Volume Observed and the Volume estimated using the model in use. 1990 to 2020.

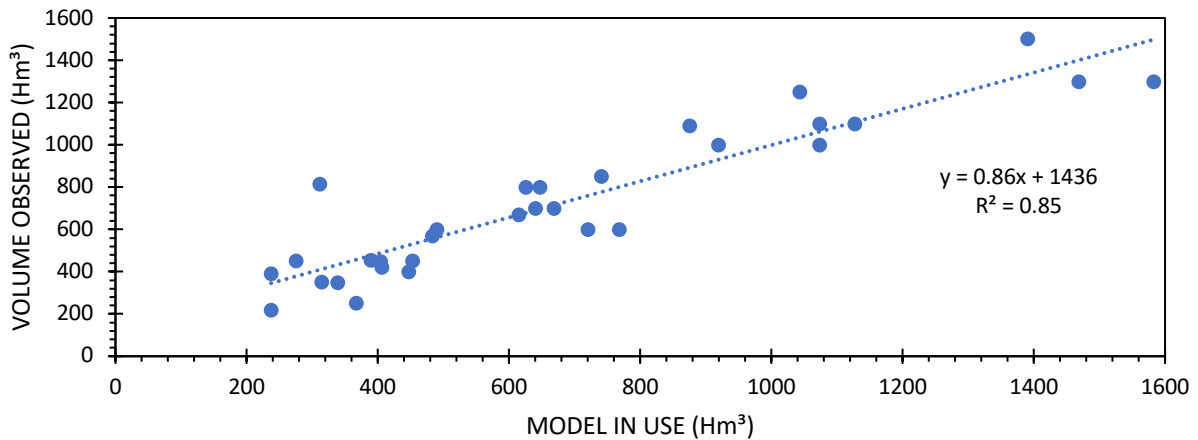


Figure 6-2: Correlation between time series of the Volume Observed and the Volume estimated using the model in use. 1990 to 2020.

The differences are mostly in the dry season or when the conditions. Seems the model in use, it cannot represent in a good manner the scarcity in the watershed, notorious is the year 2014, when the differences were very clear.

6.2 RESULTS DROUGHT ANALYSIS

To make notorious the condition and make a single characterization of the reality, about the drought situation in the watershed the methods describe in Chapter 4 are shown next. The Figure 6-3 shows the SPI values using a 12-month evaluation data from the meteorological station called Vilcuya, between 1971 and 2020, contrasted with the threshold determined by the General Directorate of Waters (-0.84 (Dry Condition)).

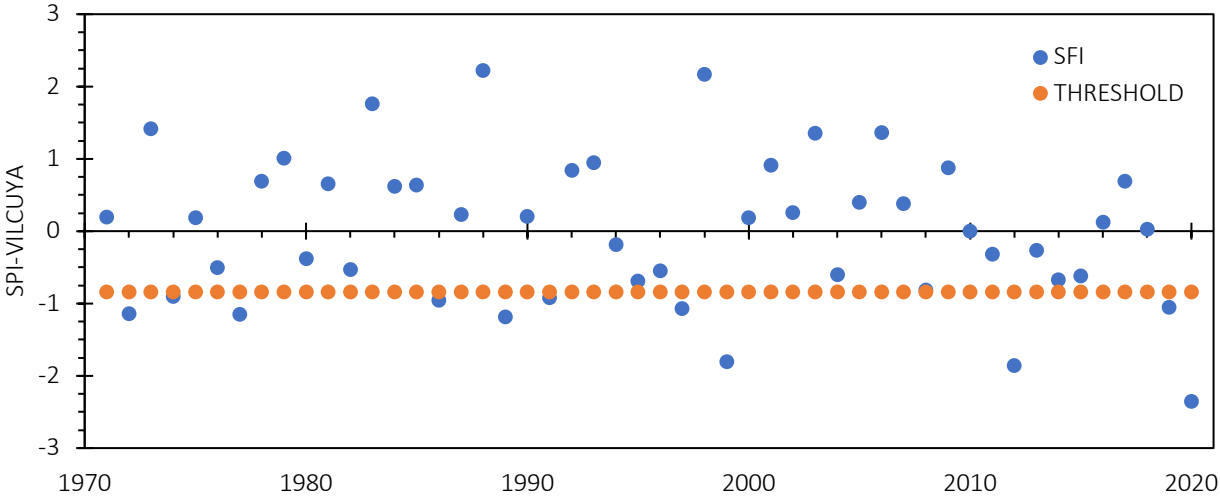


Figure 6-3: The figure shows the SPI for 12 months (blue line), between 1971-2020 for the rain station Vilcuya. The year 2019 have the lowest register of rain in the last 50 years.

The value for the SPI in the last 10 years has been under the threshold more than once and lower the threshold mostly of time since 2018, and particularly from August 2019 to May 2020, period with lowest register of precipitation in Vilcuya. This had a notorious impact in the volume for the season 2019-2020, even more, the SWE controlled was near to zero at that season. Next Figure 6-4 shows the decrease in the SPI value across the months due the lag of rain in 2019.

The SPI have an increase on May 2020, due the rain registered over that year; however, the value keeps under the threshold until December 2020, making clear the scarcity scenario in the last time and for the testing period.

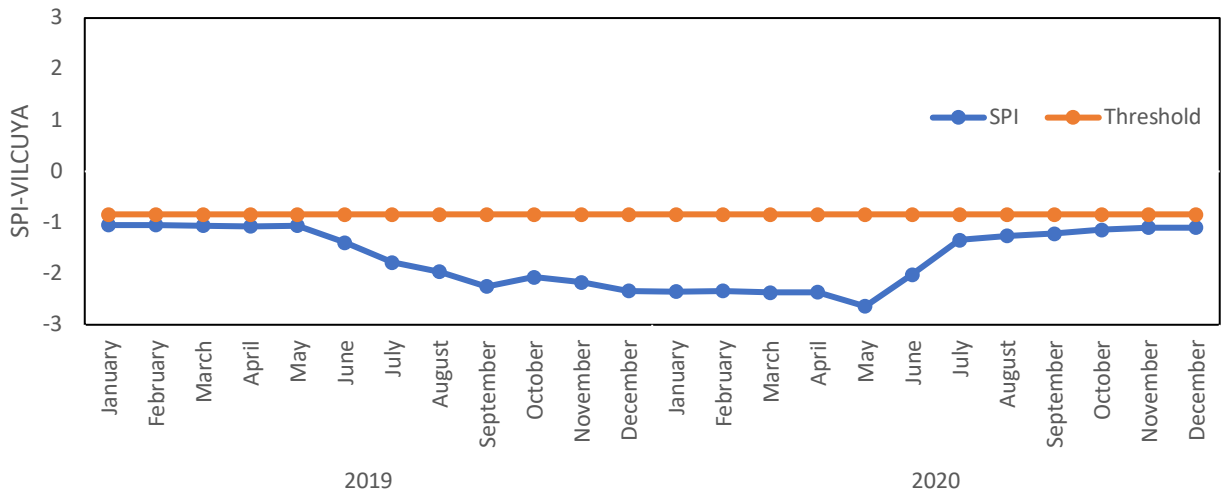


Figure 6-4: SPI for 12 months (blue line), between 2019-2020 for the rain station Vilcuya.

The values of tendencies for the Volume (Hm³), SWE (mm), Precipitation (Vilcuya) (mm) and streamflow in august (m³/s), obtained by the Mann-Kendall analysis are showed in the next table.

Table 3: Mann-Kendall results. N= 55, Years from 1965 to 2020, p=0.05.

Name	Vol (Hm ³)	SWE (mm)	Precipitation (mm)	Streamflow- August (m ³ /s)
Test Z	-2.05	-1.27	-0.639	-2.13
Significance Level				
Slope (/year)	-6.62	-4.7	-0.89	-0.139
Lower Limit	-12.79	-12.97	-3.41	-0.27
Upper Limit	-0.18	1.73	1.47	-0.01

The results of Z test and Q show a clear decreased tendency across the year. Having the Streamflow, Volume and SWE the most important and awareness fall. The decreased tendency is clear, especially from 2010, having a constant and stable behavior in the residuals since that year.

Also, to determinate the level of scarcity of volume, the next Figure 6-5 shows the adjust of the SWE, precipitation, streamflow in august and the volume statistic for a Gumbel distribution, characterizing the variables into an exceedance probability.

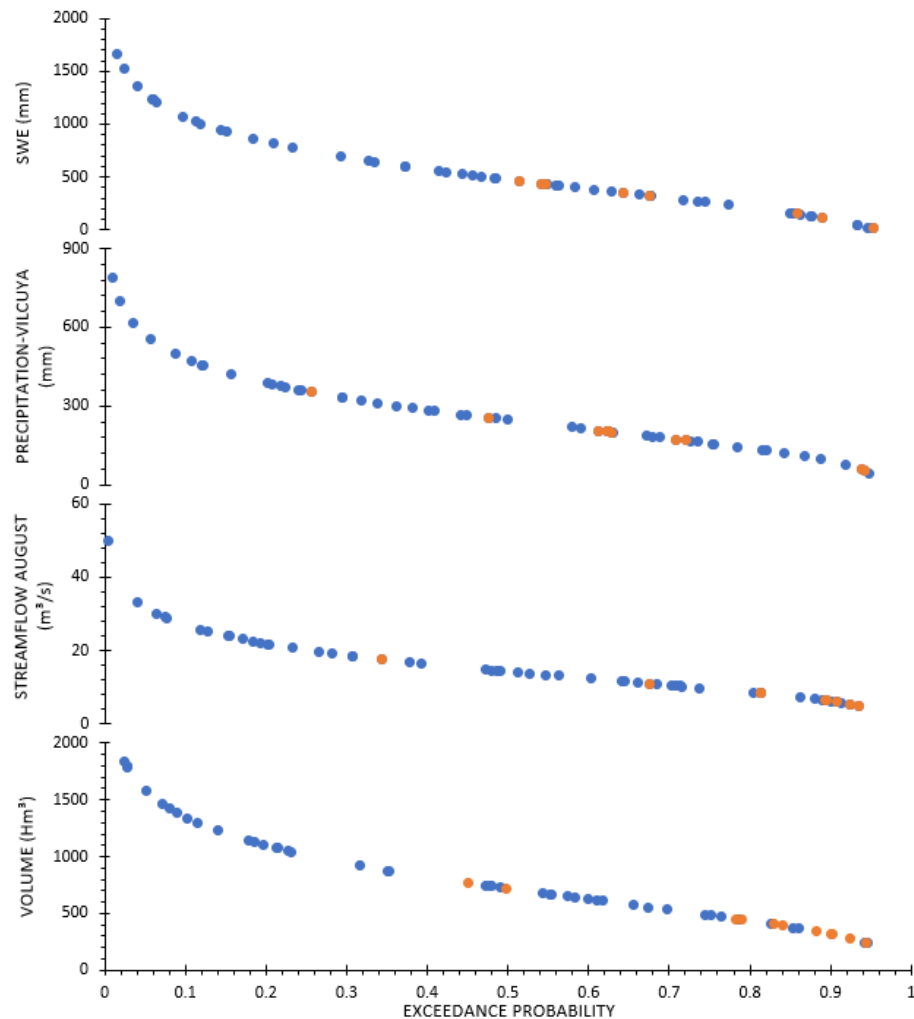


Figure 6-5: The figure shows the exceedance probability for the variables. The values in the last ten years are clearly low (orange points).

The value for the 2020 and 2019 year are about over the 70 percent of exceedance probability, which make very clear the extreme condition in the basin and in the water supply in the last years.

6.3 CORRELATIONS

To understand the relationships between the variables and the seasonal volume and generate some formulation, it needs to be analyzed as first exercise, the SWE and seasonal volume, this to evaluate the volume representation using SWE. Figure 6-6 shows the behaviors.

The next is to evaluate the rain and the volume. For this exercise, the rain from the station Vilcuya it was evaluated with volume per season. Figure 6-7 shows the correlation between these variables. Is important to understand the impacts of rain in the basin and recognize the fluctuation in the seasonal volume due changes in the rain.

The next variable to be evaluate regarding the Seasonal volume is the August runoff, which is going to be called "Start Month". August is important because gives the watershed conditions when forecast is built and because it gives the base for the forecast. The Figure 6-8 shows the correlation between these two variables.

In the figure 6-6, the data distribution shows that the problems with the SWE and Volume are in the transition's periods, from a dry season to wet season or wet to dry. The correlation is acceptable, but it needs to be improved with the rest of variables, Rain and Streamflow.

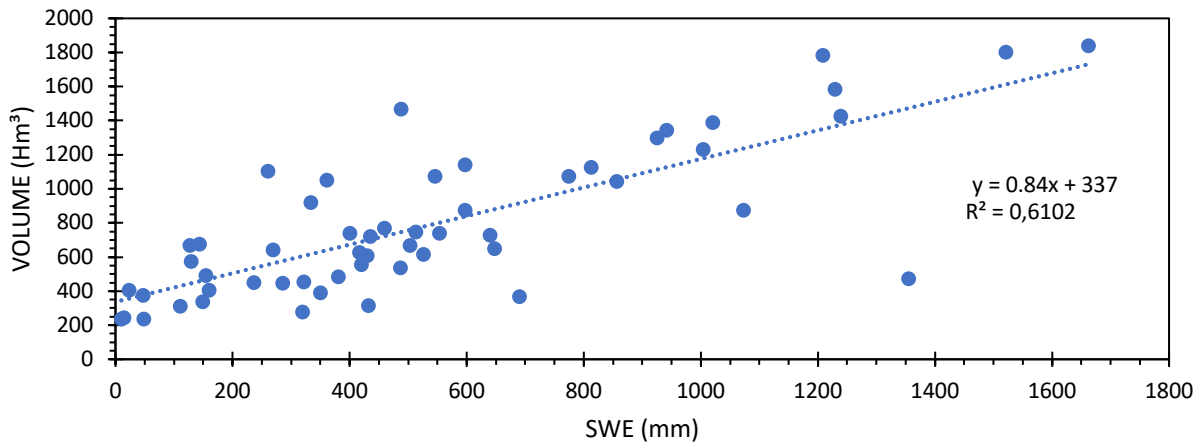


Figure 6-6: Correlation between SWE and Seasonal Volume. The graph shows some data outsiders in transitions periods. The correlation has a R^2 of 0.61.

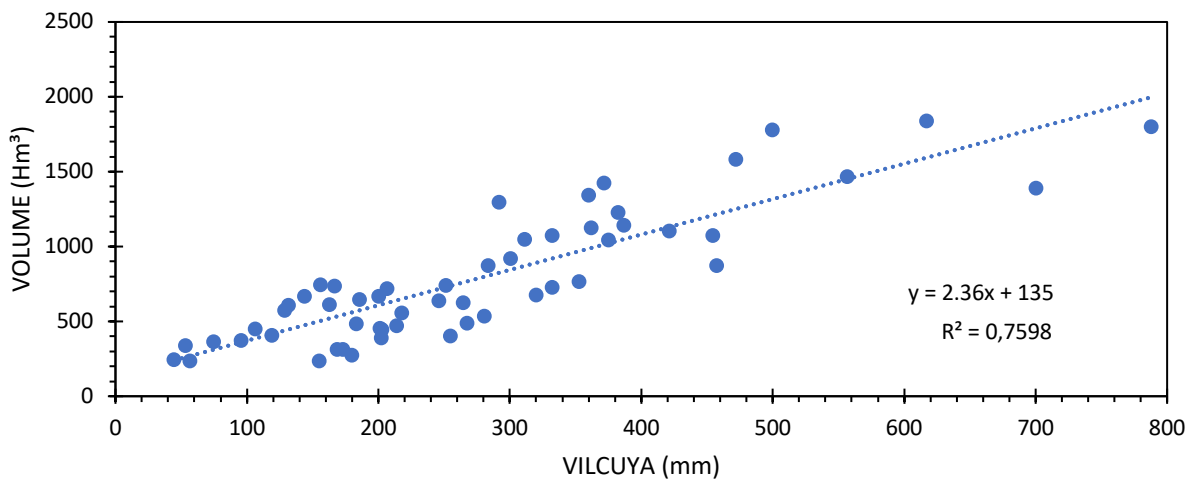


Figure 6-7: Correlation between Rain and Seasonal Volume. The correlation has a R^2 of 0.76.

The next plot shows the correlation between streamflow and volume. The correlation existing is acceptable but indicates problems in the high part of the plot, maybe because the streamflow in the wet period can change depending on the backgrounds existing.

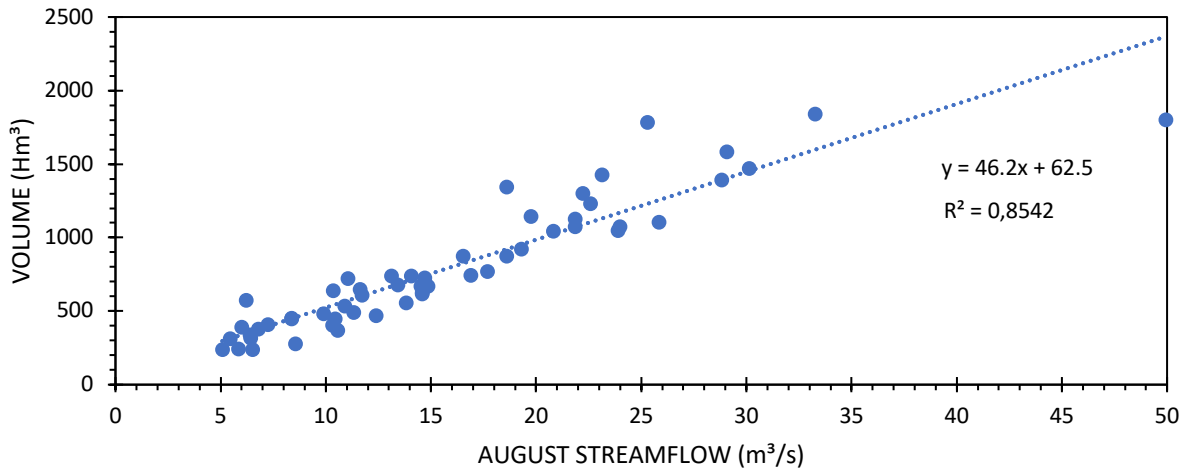


Figure 6-8: The plot shows the correlation between the August runoff and Seasonal runoff. Looks a strong relationship, with problems in the high part, problems which can be improve with the rain and SWE as inputs as well in the analysis. The correlation has a R^2 of 0.85.

Watching these relationships and correlations, seems the volume production into the watershed it's the result of influences from the rain, SWE and streamflow conditions. These main inputs will be used to explain the seasonal Volume from the flow gauge station "Río Aconcagua en Chacabuquito". Also, the variables correlation, characterize the Mediterranean nature of the basin because the runoff or volume is strongly related to the precipitations, normally concentrated in the wintertime. The figures shown the correlation between rain, SWE and Runoff with the volume. The correlation also suggests than a linear regression can improve the relationship and forecast alike.

For The Rising limb and Peak Flow, the analysis between the Start Month and each month individually between September to December it is necessary and useful. The Figure 6-9 shows an acceptable correlation between September, October, November, and December, with the Start Month.

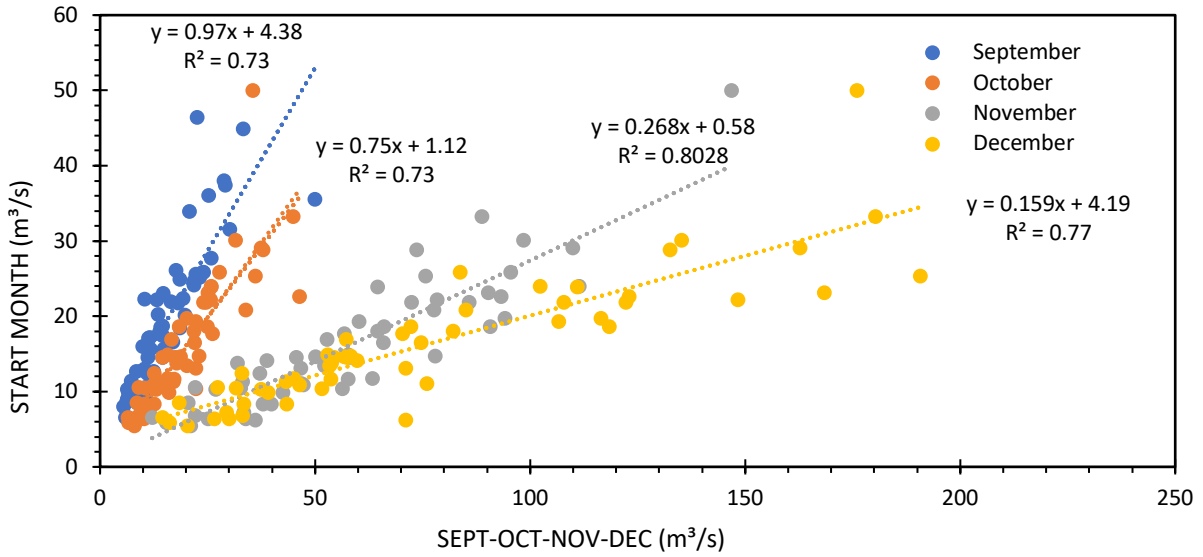


Figure 6-9: The graph shows the Start Month versus September, October, November, and December. The correlation is acceptable for each one, especially for November and December.

The Figure 6-10 shows the correlation between December and each month of the period (January, February, and March). Each correlation has an acceptable result. These correlations are an input for the recession limb construction.

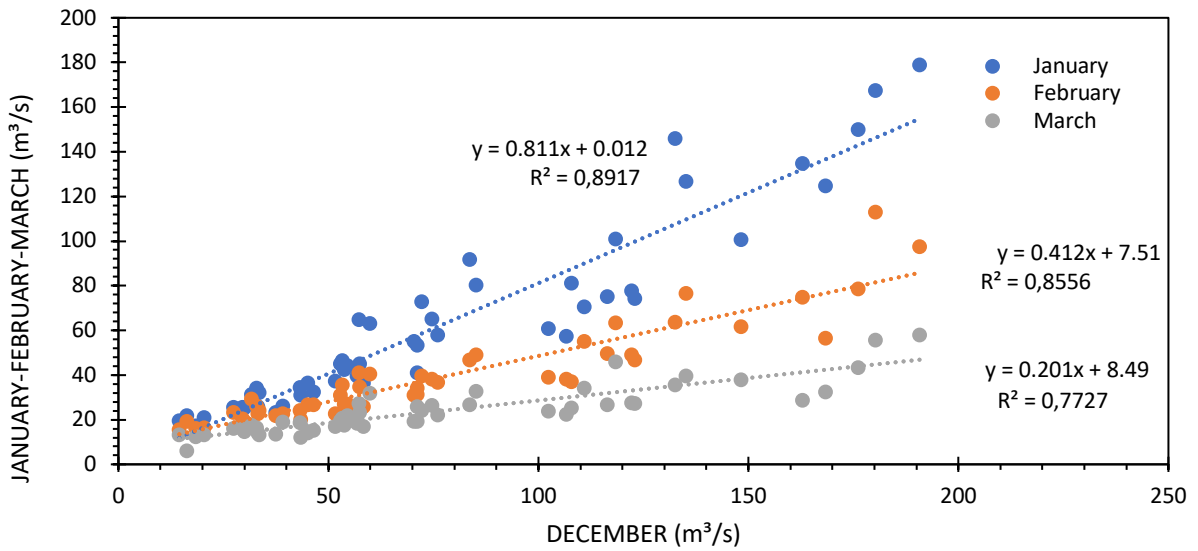


Figure 6-10: The plot shows the correlation between the December streamflow and the rest of months. The values are acceptable and use this month to forecast seems logical.

6.4 RESULTS VOLUME ESTIMATION

This section bases its results in the water heights sum of each proportion. Rain, SWE and Start Month, regarding next equation:

$$\mathbf{VOLUME\ ESTIMATED\ (mm) = RAIN\ PROPORTION\ (mm) + SWE\ PROPORTION\ (mm) + START\ MONTH\ PROPORTION\ (mm)}$$

The adjust made for the RAIN PROPORTION, finally used only two stations from the original pool of three, due the regression analysis. The station discarded for estimation it was Los Andes. For this reason, the equation used for this proportion it is as follow:

$$\mathbf{RAIN\ PROPORTION\ (mm) = a * Vilcuya\ (mm) + b * Riecillos\ (mm)}$$

a	0.26
b	0.06

The adjust made for SWE PROPORTION, have the next value for the parameter:

$$\mathbf{SWE\ PROPORTION\ (mm) = c * SWE\ Portillo\ (mm)}$$

c	0.08
---	------

The adjust made for the START MONTH PROPORTION, have the next value for the parameter:

$$\mathbf{START\ MONTH\ PROPORTION\ (mm) = d * START\ MONTH\ (mm)}$$

d	4.55
---	------

Table 4: Results Seasonal Volume.

TESTING PERIOD-VOL (Hm ³)		
YEAR	CONTROLLED	ESTIMATED
2011	393	395
2012	447	468
2013	453	464
2014	312	307
2016	768	883
2017	404	534
2020	390	403

Table 5: NSE. Results Seasonal Volume.

NASH-SUTCLIFFE - TESTIN PERIOD	0.83
--------------------------------	------

6.5 RESULTS RISING LIMB AND PEAK FLOW

$$\text{Monthly Percentage} = \alpha \frac{\text{Volume Start Month Season } i}{\text{Volume Season } i} + \beta \frac{\text{August Temperature Season } i}{\text{Monthly Average Temp Month}}$$

Table 6: Parameters Rising limb and Peak Flow.

Parameter	Sept	Oct	Nov	Dec
α	0.594	0.504	1.306	1.4851E-05
β	0.038	0.112	0.184	0.429

Table 7: Average Monthly Temperatures.

Average Monthly Temp (°C)			
Sept	Oct	Nov	Dec
12.2	14.5	17.0	19.4

Table 8: Results Rising Limb-Peak Flow.

RISING LIMB-PEAK FLOW (m³/s)				
YEAR	SEPT	OCT	NOV	DEC
2011	10	18	29	40
2012	12	20	34	44
2013	12	21	35	47
2014	9	16	26	37
2016	26	44	75	98
2017	14	24	40	51
2020	10	18	29	41

Table 9: NSE. Results Rising Limb-Peak Flow.

NASH-SUTCLIFFE - TESTING PERIOD	0.79
---------------------------------	------

6.6 RESULTS RECESSION LIMB

$$y' = \alpha Qd$$

Table 10: Parameters Recession Limb

Parameter	Jan	Feb	Mar
α	1.418	2.041	2.432

Table 11: Results Recession Limb.

FALLING LIMB (m ³ /s)-FIRST APPROACH				DEC-OBSERVED	FALLING LIMB (m ³ /s)-CORRECTION		
YEAR	JAN	FEB	MAR		JAN	FEB	MAR
2011	32	19	11	30	24	14	9
2012	35	21	13	33	26	16	10
2013	37	22	13	43	34	21	12
2014	29	18	11	20	16	10	6
2016	78	47	28	70	56	34	20
2017	40	24	14	37	30	18	11
2020	32	20	12	26	21	13	8

Table 12: NSE. Results Recession Limb.

NASH-SUTCLIFFE - TESTING PERIOD	0.72
NASH-SUTCLIFFE - TESTING PERIOD CORR.	0.79

6.7 RESULTS FIRST APPROACH AND CORRECTION

For this section, the result evaluated it will consider the first approach and the correction made with the controlled streamflow in December.

Table 13: Results First Approach.

YEAR	SEPT	OCT	NOV	DEC	JAN	FEB	MAR	SUM VOL
2011	10	18	29	40	32	19	11	420
2012	12	20	34	44	35	21	13	472
2013	12	21	35	47	37	22	13	493
2014	9	16	26	37	29	18	11	383
2016	26	44	75	98	78	47	28	1043
2017	14	24	40	51	40	24	14	545
2020	10	18	29	41	32	20	12	424

Table 14: Results. Correction Made with December Streamflow Controlled

YEAR	SEPT	OCT	NOV	DEC- OBSERVED	JAN	FEB	MAR	SUM VOL
2011	10	18	29	30	24	14	9	351
2012	12	20	34	33	26	16	10	399
2013	12	21	35	43	34	21	12	472
2014	9	16	26	20	16	10	6	272
2016	26	44	75	70	56	34	20	854
2017	14	24	40	37	30	18	11	456
2020	10	18	29	26	21	13	8	326

Table 15: Results Volume.

TESTING PERIOD VOL (Hm ³)			
YEAR	OBSERVED	ESTIMATED	ESTIMATED - CORRECTED
2011	393	420	351
2012	447	472	399
2013	453	493	472
2014	312	383	272
2016	768	1043	854
2017	404	545	456
2020	390	424	326

Table 16: NSE. Results Volume.

NASH-SUTCLIFFE - TESTING PERIOD	0.70
NASH-SUTCLIFFE - TESTING PERIOD CORR.	0.91

Table 17: Observed Streamflow per month and per season, and the observed Volume per season (SUM VOL).

OBSERVED STREAMFLOW (m ³ /s) AND VOLUME (Hm ³)								
YEAR	SEPT	OCT	NOV	DEC	JAN	FEB	MAR	SUM VOL
2011	10	16	34	30	25	19	15	393
2012	13	15	40	33	32	24	13	447
2013	10	18	38	43	31	20	12	453
2014	8	19	21	20	21	16	13	312
2016	26	34	57	70	55	31	19	768
2017	13	18	27	37	23	22	13	404
2020	9	20	27	26	22	23	19	390

7 DISCUSSION

The method and model are producing good results especially in dry scenarios (Table 6-12), which have become the norm for most of the last decade in the basin. The drought analysis identified these drought conditions since 2010 (Figure 6-3), which is considered a megadrought (Boisier *et al.*, 2016). These conditions are affecting the results from the model in use, especially when dry conditions are consistent (Fassnacht *et al.*, 2004) while stationarity is assumed (Valdes-Pineda *et al.*, 2014).

7.1 DISCUSSION MODEL IN USE VS OBSERVED VOLUME

The model in use by the General Directorate of Waters has not working well since 2010 (Figure 6-1), when the megadrought started. The Figure 6-1 shows the differences with the observed values, which are significances when a dry season occurs and the hydrological predictability is difficult to represent (Pagano *et al.*, 2014). The model in use needs to be improved, incorporating new climate conditions represented by more recent data, including the last ten years of information measured across the watershed, which can relate in a better way the scarcity and runoff modes into the basin (Reinsfield *et al.*, 2014).

The model in use is also failing to produce an adequate distribution in streamflow across the season, which is important information required by water managers and operators (Pagano *et al.*, 2014). While the volume estimates/forecasts are very similar to those observed, but the distribution is not well represented in terms of the timing of peak flows and for recession flows, as is observed in Figure 9-1 and Figure 9-2, Appendix.

7.2 DISCUSSION DROUGHT ANALYSIS

The drought analysis shows a drought condition for many of the last ten years (Figure 6-3), especially for the 2010-2011 and 2019-2020 season (Figure 6-4), when the low rain and SWE affected the monthly runoff and seasonal volume. The values for the SPI method (WMO, 2012) using 12-months evaluation (WMO, 2012), show a very stressed situation in 2019 (Figure 6-4) since the forecasted value was below the legal drought condition threshold determined by the DGA (Código de Aguas, 1981). The SPI method provides a good characterization for such conditions (Mckee *et al.*, 1993). A similar assessment of a streamflow could be undertaken to evaluate how the decline in rain influences runoff.

The trend analysis shows a decrease in runoff volume, SWE, and precipitation (Table 6-1); only the decrease in runoff volume and precipitation at Riecillos are statistically significant, based on the Mann-Kendall test (Gilbert, 1987). Decreases have been seen in the snowpack across much of the Andes over the past two decades (Malmros *et al.* 2018; Saavedra *et al.*, 2018; Cordero *et al.*, 2019), which is similar to what has been seen for the snowpack in many parts of the globe (Huning & AghaKouchak, 2020).

The frequency analysis using the Gumbel Distribution illustrates that the last three seasons runoff volumes have an exceedance probability of around 70 percent, which mean is a phenomenon non-recurrent (Naghetini, 2017), this also support the conclusion of the extreme condition and drought registered and lived until now. The value for 2019-2020 season is the lower value in the last ten years with about a 90 percent of the exceedance probability

(Fassnacht *et al.*, 2004), which also needs to be re-evaluated, to conclude the impact in future designs and developments.

7.3 DISCUSSION VOLUME ESTIMATION

The volume estimated by the new method is a good approximation to the observed volume (Table 6-2), especially in seasons with limited water availability. This supports the use Parsimonious models to address such objectives (Pagano *et al.*, 2014). For this exercise, the calibration period included the 2019-2020 season as an input. The results for the testing period had a NSE value of 0.83, which implies that the model's results are acceptable (Moriasi *et al.*, 2007). Also is important to note that the variables with the most impact on the volume estimation are the precipitation at Vilcuya and the Runoff of August or Start Month. The model also is using individual process relationships to constrain the model behavior (Nearing & Gupta, 2018), which makes it easier to qualify and weight of each variable into the model.

7.4 DISCUSSION RESULTS RISING LIMB AND PEAK FLOW

The results from this assessment are acceptable (Table 6-11), with a NSE of 0.79 for the testing period. Yet, the problems are in the month of November and December with poorer estimates for these months. Compared to the other months, this is peak flow and the characteristics in this part of the hydrograph is complicated to model, often since modeling can be dependent on variables that were not incorporated into the model or for the forecasting time (Follum *et al.*, 2019). For this reason, some results have differences with the observed data, and particularly the results estimated for the seasons 2016-2017 and 2020-2021, when the differences, especially in the peak flow, are important, which can be a lack in the information for

water management into the watershed (Pagano, 2014). However, the new model can update the input data, and re-evaluate the forecast in the middle of the season.

7.5 DISCUSSION RESULTS RECESSION LIMB

The values forecasted for the recession limb are good and are as expected for this part of the hydrograph (Table 6-11), especially when the model is updated during the forecast season (Thomas *et al.*, 2015). This is especially true when updates occur with December streamflow values. The NSE for the first approximation using the estimated value for December is 0.72 and this increases to 0.79 when the model is re-evaluated with the December streamflow. The model provides the worse estimates for March (Table 6-12). Further analysis using other variables could improve the recession limb.

7.6 DISCUSSION SET MODEL AND CORRECTION

The “model set” is the last part of the method, the construction of the values for the first approach are generating good values for the NSE of 0.70; when the correction is made, the NSE value increases to 0.91 (Table 6-12). The shape of the hydrograph resembles a normal distribution across the season. This method can be automated since the input variables are available electronically in near real-time. This can help generate the forecasts to allow for more time in analyzing the estimates (Pagano *et al.*, 2014). The model can be operated and inserted in an automatic process, and also have tools to generate changes for re-evaluation between January and March (Pagano *et al.*, 2014). However, the next step is to incorporate the complete time series into the calibration process, which should improve the results considering that it would include a large range of scenarios, especially extended dry periods (Boisier *et al.*, 2016).

The problems with the current methods are highlighted in periods of drought (Fassnacht *et al.*, 2004). Due to drought, the timing of the peak in the hydrograph tends to change; for example, in the 2010-2011 season, peak flows under a dry condition occur in November while typically the peak occurs in December (Figure 7-1). In such conditions, model updates in December may not be as useful as November updates. This may require model modifications, since flows are already receding in December in dry years, such as 2010-2011 (Figure 7-1). This method obviously can be improved with other tools and methods to include other components (Follum *et al.*, 2019).

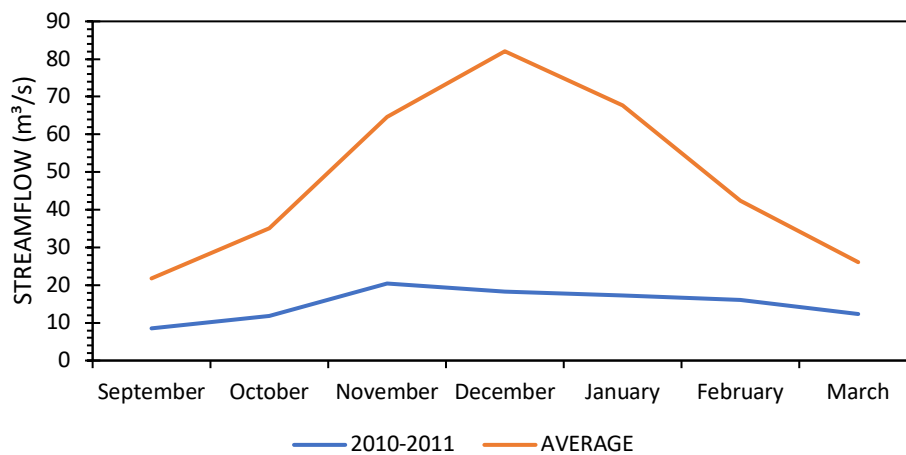


Figure 7-1 Monthly streamflow in the season 2010-2011 (driest in 30 years) versus the average streamflow.

8 CONCLUSIONS

The study presented the correlation between variables, and different climatic conditions. The dry and wet scenarios, i.e., extreme values, have a strong impact on the results. The new analysis compensates for some of the previously differences between observed and estimated runoff volume.

A long-term (50+ year) record of data it was used. This builds upon the historical correlation between streamflow and SWE, and other variables, over a variety of climatic scenario. These conditions will reflect many of the future conditions. The volume estimated under this method is quite similar to the observed values, but differences persist under stressed conditions, particularly during drought or scarcity conditions, such as observed from 2010 to 2015, and from 2018 to 2020.

The streamflow estimated for the study period represents the observed streamflow well, and the new model should provide useful forecast information. The main problem is representing the peak flow correctly in November versus December; the model was created for normal condition which has the peak in December. However, the re-evaluation tool can improve the differences observed, especially for the recession limb.

The model can be used in a manual or automatic manner, especially the construction of the hydrograph, which is very easy to understand and to improve with new techniques and other variables.

9 FUTURE WORK AND RECOMENDATIONS

Future work could improve results by further differentiating between normal, dry, and wet periods. This characterization should improve the volume estimation and the determination of peak flow. During an average season, the models work very well, while under an extreme scenario the results can be acceptable, they are dependent on the prior conditions existing in the watershed.

The use of more data could be beneficial. The flow gauge station has almost 100 years of data and the SWE station started in 1951. Such lengthening of the data record would introduce addition hydro-climatic scenarios. In Figure 3-4, the SWE data across the time have notorious changes and tendencies between years, especially the years 1968 and 2019, the driest years in the records. Decrease related with the streamflow on those seasons. But, beyond correlating streamflow and SWE, the assessment could also include trend analysis and frequency analysis for extremes.

This analysis should be regularly reevaluated, such as every 10 years to incorporate the data and information from the new hydro-climatic conditions. The model uses input from every time step, i.e., every year, but considering the drought conditions over the last decade, it seems logical to revisit the model with any new, extreme conditions.

10 REFERENCES

Ahmadi M, Arabi M, Ascough II j, Fontane D, Engel B. 2014. Toward improved calibration of watershed models: Multisite multiobjective measures of information. *Environmental Modelling and Software*, 59(2014), 135-145. <http://dx.doi.org/10.1016/j.envsoft.2014.05.012>

Aravena, J., Luckman, B. 2008. Spatio-temporal rainfall patterns in Southern America. *International Journal of Climatology*, **29**: 2106-2120 (2009). DOI: 10.1002/joc.1761.

Arsenault R, Brissette F. 2013. Determining the Optimal Spatial Distribution of Weather Stations Networks for Hydrological Modeling Purpose Using RCM datasets: An Experimental Approach. American Meteorological Society. 2014. DOI: 10.1175/JHM-D13-088.1.

Barcaza G, Nussbaumer S, Tapia G, Valdes J, Garcia JL, Videla Y, Albornoz A, Arias V. 2017. Glacier inventory and recent glacier variations in the Andes of Chile, South America. *Annals of Glaciology* 58(75pt2)2017. DOI: 10.1017/aog.2017.28.

Benitez A, Aylwin L. 1976. Estudio de Previsión de Escurrimientos de Deshielo. División de Estudios. Empresa Nacional de Electricidad SA. <https://snia.mop.gob.cl/sad/CDA2616.pdf>

Boisier JP, Rondanelli R, Garreaud R, Munoz F. 2016. Anthropogenic and natural contributions to the Southeast Pacific precipitation decline and recent megadrought in central Chile. *Geophys. Res. Lett.*, **43**, 413-421. DOI: 10.1002/2015GL067265.

Bown F, Rivera A, Acuña C. 2008. Recent glacier variations at the Aconcagua basin, central Chile Andes. *Annals of Glaciology*, **48**, 2008.

Bradley RS, Vuille M, Diaz HF, Vergara W. 2006. Threats to water supplies in Tropical Andes. *Science* **312**: 1755-1756.

Bravo C, Loriaux T, Rivera A, W. Brock B. 2017. Assessing glacier melt contribution to streamflow at Universidad Glacier, central Andes of Chile. *Hydrol. Earth Syst. Sci.*, 21, 3249-3266, 2017. DOI: 10.5194/hess-21-3249-2017.

Buisson L, Blanc G, Grenoillet G. 2008. Modelling stream fish species distribution in a river network: the relative effects of temperature versus physical factors. *Ecol. Freshwater. Fish.* 17, 244-257.

Carrasco J, Casassa G, Quintana J. 2005. Changes of the 0°C isotherm and the equilibrium line altitude in central Chile during the last quarter of the 20th century. *Hydrological Sciences Journal*, 50:6,-948. DOI: 10.1623/hysj.2005.6.933.

Código de Aguas, Derecho de Aprovechamiento de Aguas, Aguas/legislación/Chile. 1981.
<https://www.bcn.cl/leychile/navegar?idNorma=5605>

Collados-Lara A-J, Fassnacht SR, Pulido-Velazquez D, Pfohl AKD, Morán-Tejeda E, Venable NBH, Pardo-Igúzquiza E, Puntteney-Desmond E. 2021. Intra-day variability of temperature and its near-surface gradient with elevation over mountainous terrain: comparing MODIS Land Surface Temperature data with coarse and fine scale near-surface measurements. *International Journal of Climatology*, 41(S1), E1435-E1449. DOI: 10.1002/joc.6778

Dunne T, Leopold L. 1978. *Water in Environmental Planning*. San Francisco, CA: W.H. Freeman.

Durance I, Ormerod S. 2009. Trends in water quality and discharge confound long-term warming effects on river macroinvertebrates. *Freshwater. Ecol.* 54, 388-405.

Erickson T, Stefan H. 1996. Correlation of Oklahoma stream temperatures with air temperatures. University of Minnesota, St. Anthony Falls Laboratory, Project Report No. 398, Minneapolis, MN.

Fassnacht SR, Soulis ED, Kouwen N. 1999. Algorithm application to improve weather radar snowfall estimates for winter hydrologic modelling. *Hydrological Processes*, 13(18), 3017-3039. DOI: 10.1002/(SICI)1099-1085(19991230)13:183.O.CO;2-K

Fassnacht SR, Dressler KA, Bales RC. 2003. Snow water equivalent interpolation for the Colorado River Basin from snow telemetry (SNOTEL) data. *Water Resources Research*, 39(8), 1208. DOI: 10.1029/2002WR001512.

Fassnacht SR, Yusuf F, Kouwen N. 2004. Paralyzing January 1999 snowstorm produced minimal streamflow for Southern Ontario. *Canadian Water Resources Journal*, 29(1), 1-12. <https://doi.org/10.4296/cwrj1>

Fassnacht SR, Deitemeyer DC, Venable NBH. 2014. Capitalizing on the daily time step of snow telemetry data to model the snowmelt components of the hydrograph for small watersheds. *Hydrol. Process.* **28**, 4654-4668 (2014). DOI: 10.1002/hyp.10260.

Follum M, Niemann J, Fassnacht S. 2019. A comparison of snowmelt-derived streamflow from temperature-index and modified-temperature-index snow models. *Hydrological Processes* 2019; 33:3030-3045. DOI: 10.1002/hyp.13545.

Francou B, Vuille M, Wagnon P, Mendoza J, Sicart JE. 2003. Tropical climate change recorded by a glacier in the central Andes during the last decades of the twentieth century: Chacaltaya, Bolivia. *Journal of Geophysical Research* vol. 108, D5, 4154: 1-12.

Garcia-Ruiz J, Lopez-Moreno J, Vicente-Serrano S, Lasanta-Martinez T, Bergueria S. 2011. Mediterranean water resources in a global change scenario. *Earth Sci Rev*, 105(3-4):121-139.

Garreaud R, Alvarez-Garreton C, Barichivich J, Boisier JP, Duncan C, Galleguillos M, LeQuense C, McPhee j, Zambrano-Bigiarini M. 2017. The 2010-2015 megadrought in central Chile: impacts on regional hydroclimate and vegetation. *Hydrology and Earth System Sciences; Katlenburg-Lindau*, 21(12), 6307-6327. <https://doi.org/http://dx.doi.10.5194/hess-21-6307-2017>

Garreaud RD. 2009. The Andes climate and weather. *Adv. Geosci.*, 22, 3-11,2009.

Gilbert RO. 1987. *Statistical Methods for Environmental Pollution Monitoring*. Van Nostrand Reinhold, New York, NY, 336pp.

Gonzalez S, Garreaud R. 2019. Spatial variability of near-surface temperature over the coastal mountains in southern Chile (38°S). *Meteorol Atmos Phys* (2019), 131:89-104. <https://doi.org/10.1007/s00703-017-0555-4>

Hamed KH. 2007. Trend detection in hydrological data: The Mann-Kendall trend test under the scaling hypothesis. *Journal of Hydrology*, **349** (2008), 350-363. DOI: 10.1016/j.jhydrol.2007.11.009.

Hammond J, Kampf S. 2020. Subannual streamflow responses to rainfall and snowmelt inputs in snow-dominated watershed of the western United States. *Water Resources Research*, 56, e2019WR026132. DOI: 10.1029/2019WR026132

Harpold A, Kaplan M, Zion Klos P, Link T, McNamara J, Rajagopal S, Schumer R, Steele C. 2016. Rain or snow: hydrologic processes, observations, prediction and research needs. *Hydrol. Earth Syst. Sci.*, 21, 1-22, 2017. DOI: 10.5194/hess-21-1-2017

Huning L, AghaKouchak A. 2020. Global snow drought hot spot and characteristics. *PNAS*. August 18, 2020. Vol. 117. no 33. 19755. DOI: 10.1073/pnas.1915921117

Joo H, Lee J, Jun H, Kim K, Hong S, Kim J, Soo Kim H. 2019. Optimal Stream Gauge Network Design Using Entropy Theory and Importance of Stream Gauge Stations. *Entropy*, 21, 991. DOI: 10.3390/e21100991.

MacDonald R, Boon S, Byrne J. 2014. A process-based stream temperature modelling approach for mountain regions. *Journal of Hydrology*, 511 (2014), 920-931.

Martinez J, Rango A, Roberts R. 2008. *Snowmelt Runoff Model (SRM) User's Manual* (eds) Gomez-Landesa E and Bleiweiss M P; New Mexico State University, Las Cruces, NM.

Masiokas NH, Villalba R, Luckman BH, Montaña E, Betman E, Christie D, Le Quesne C, Mauget S. 2013. Recent and Historic Andean Snowpack and Streamflow Variations and Vulnerability to Water shortages in Central-Western Argentina. In *Climate Vulnerability*, Pielke RA (ed). Academic Press: Oxford and New York, NY, 231-227, DOI: 10.1016/b978-0-12-384703-4.00522-0.

McCuen R, Knight Z, Cutter G. 2006. Evaluation of the Nash-Sutcliffe Efficiency Index. *J. Hydrol. Eng.*, 2006, 11(6): 597-602.

McKee T, Doesken N, Kleist J. 1993. The relationship of drought frequency and duration to time scale. Boston, American Meteorological Society, 179-184.

McMillan H, Seibert J, Petersen -Overleir A, Lang M, White P, Snelder T, Rutherford K, Krueger T, Mason R, Kiang J. (2017), How uncertainty analysis of streamflow data can reduce costs and promote robust decisions in water management applications, *Water Resour. Res.*, 53, 5220–5228, DOI:10.1002/2016WR020328.

Mekonnen M, Hoekstra A. 2016. Four billion people facing severe water scarcity. *Science Advance*, 2(2), e1500323.

Meybeck M, Green P, Vorosmarty CJ. 2001. A new typology for mountains and other relief classes: An application to global continental water resources and population distribution, *Mt. Res. Dev.*, 21(1), 34-45.

Milella P, Bisantino T, Gentile F, Iacobellis V, Liuzzi GT. 2012. Diagnostic analysis of distributed input and parameter datasets in Mediterranean basin streamflow modeling. *Journal of Hydrology*, 742-743, 262-276.

Misha A, Coulibaly P. 2009. Developments in hydrometric network design: A review, *Rev. Geophys.*, 47, RG2001. DOI: 10.1029/2007RG000243.

Mohseni O, Stefan H. 1999. Stream temperature/air temperature relationship: a physical interpretation. *Journal of Hydrology*, 218 (1999), 128-141.

Moriasi, D. N., Arnold, J. G., Van Liew, M. W., Bingner, R. L., Harmel, R. D., and Veith, T. L.: Model evaluation guidelines for systematic quantification of accuracy in watershed simulations, *Trans. ASABE*, 50, 885–900, 2007.

Moussa R, Chahinian N, Bocquillon C. 2007. Distributed hydrological modeling of a Mediterranean mountainous catchment-model construction and multi-site validation. *Journal of Hydrology*, 337, 35-51.

Naghattini M. 2017. *Fundamentals of Statical Hydrology*. Springer 2017. DOI: 978-3-319-43560-2

Nearing GS, Gupta HV. 2018. Ensembles vs. information theory: supporting science under uncertainty. *Front. Earth Sci.*, 12, 653–660. DOI: 10.1007/s11707-018-0709-9

Niemeyer J, Link T, Seyfried M, Flerchinger G. 2016. Surface water input from snowmelt and rain throughfall in western juniper: potential impacts of climate change and shifts in semi-arid vegetation. *Hydrol. Process.* **30**, 3046-3060 (2016). DOI: 10.1002/hyp.10845.

Oki T, Kanae S. 2006. Global hydrological cycles and world water resources. *Science*, 313 (5790), 1068-1072.

Pagano T, Garen D, Sorooshian S. 2004. Evaluation of Official Western U.S. Seasonal Water Supply Outlooks, 1922-2002. *Journal of Hydrometeorology*, Vol. 5, 2004.

Pagano T, Wood A, Ramos MH, Cloke H, Pappenberger, Clark M, Cranston M, Kavetsky D, Mathevet T, Sorooshia S, Verkade J. 2014. Challenge of Operational River Forecasting. *Journal of Hydrometeorology*, Vol3 15,2014. DOI: 10.1175/JHM-D-13-0188.1

Painter T, Skiles S, Deems J, Brandt W, Dozier J. 2018. Variation in rising limb of Colorado River snowmelt runoff hydrograph controlled by dust radiative forcing in snow. *Geophysical Research Letters*, 45, 797-808. <https://doi.org/10.1002/2017GL075826>.

Peduzzi P, Herold C, Silveiro W. 2010. Assessing high altitude glacier thickness, volume and area changes using field, GIS and remote sensing techniques: the case of Nevado Coropuna (Peru). *The Cryosphere* 4(3): 313-323, DOI: 10.5194/tc-4-313-2010.

Peña H, Nazarala B. Snowmelt runoff simulation model of a central Chile Andean basin with relevant orographic effects, in: *Large Scale Effects of Seasonal Snow Cover*, IAHS Publ. No. 166, Vancouver, Canada, 1987.

Perez C, Nicklin C, Dangles O, Vanek S, Sherwood S. 2010. Climate Change in the High Andes: Implications and Adaptation Strategies for Small-scale Farmers. *The International Journal of Environmental, Cultural, Economic and Social Sustainability* Volume 6, 2010, <http://www.Sustainability-Journal.com>, ISSN1832-2077

Phoung J, Bandaragoda C, Instanbulluoglu E, Beveridge C, Strauch R, Setiawan L, Mooney S. 2019. Automated retrieval, preprocessing, and visualization of gridded hydrometeorology data products for spatial-temporal exploratory analysis and intercomparison. *Eviron. Model. Softw.* 116. 119-130.

Rabatel A, Francou B, Soruco A, Gomez J, Caceres B, Ceballos JL, Basantes R, Vuille M, Sicart JE, Huggel C, Scheel M, Lejeune Y, Arnaud Y, Collet M, Condom T, Consoli G, Favier V, Jomelli V, Galarraga R, Ginot P, Maisincho L, Mendoza J, Menegoz M, Ramirez E, Ribstein P, Suarez W, Villacis M, Wagnon P. 2013. Current state of glaciers in the tropical Andes: a multi-century

perspective on glacier evolution and climate change. *The Cryosphere* **7**(1): 81-102, DOI: 10.5194/tc-7-81-2013.

Reinsfield I, Swanson E, Cohen T, Larsen J, Nolan A. 2014. Hydrospatial assessment of streamflow yields and effects of climate change: Snowy Mountains, Australia. *Journal of Hydrology*, 512 (2014), 206-220.

Rutlant J, Fuenzalida H. 1991. Synoptic aspects of the central Chile rainfall variability in southern South America. *International Journal of Climatology*, **11**(1), 63-76.

Saavedra, F., Kampf, S., Fassnacht, S., Sibold, J. 2016. A snow climatology of the Andes Mountains from MODIS snow cover data. *International Journal of Climatology*. **37**: 1526-1539 (2017). DOI: 10.1002/joc.4795.

San Miguel-Vallelado A, Moran-Tejeda E, Alonso-Gonzalez E, Lopez-Moreno J. 2017. Effect of snow on mountain river regimes: an example from the Pyrenees. *Front. Earth Sci.* 2017, 11(3): 515-530. DOI: 10.1007/s11707-016-0630-z.

Sexstone G, Fassnacht S. 2014. What drives basin scale spatial variability of snowpack properties in northern Colorado? *The Cryosphere*, 8, 329-344, 2014. DOI: 10.5194/tc-8-329-2014

Tahir A, Chevallier P, Arnaud Y, Neppel L, Ahmad B. 2011. Modelling snowmelt-runoff under climate scenarios in the Hunza River basin, Karakoram Range, northern Pakistan. *Journal of Hydrology*, **409**(1-2), 104-117.

Tasdighi A, Arabi M, Harmel D, Line D. 2018. A Bayesian total uncertainty analysis framework for assessment of management practices using watershed models. *Environmental Modelling and Software*, 108 (2018), 240-252. <https://doi.org/10.1016/j.envsoft.2018.08.006>

Thomas B, Vogel R, Famiglietti J. 2015. Objective hydrograph baseflow recession analysis. *Journal of Hydrology*, 525(2015), 102-112. <http://dx.doi.org/10.1016/j.jhydrol.2015.03.028>.

Valdes-Pineda R, Pizarro R, García-Chevesich P, Valdes J, Olivares C, Vera M, Balocchi F, Perez F, Vallejos C, Fuentes R, Abarza A, Helwig B. 2014. Water governance in Chile: Availability, management, and climate change. *Journal of Hydrology* 519 (2014), 2538-2567.

Viviroli D, Durr H, Messerli B, Meybeck M, Weingartner R. 2007. Mountains of the world, water towers for humanity: Typology, mapping, and global significance. *WATER RESOURCES RESEARCH*, VOL. 43, W07447. DOI: 10.1029/2006WR005653.

Webb M, Winter J, Spera S, Jonathan W, Chipman & Osterberg E. 2020. Water, agriculture, and climate dynamics in central Chile's Aconcagua River Basin, *Physical Geography*. DOI: 10.1080/02723646.2020.1790719.

Whitaker A, Sugiyama H, Hayakawa K. 2008. Effect of snow cover conditions on the hydrologic regime: case study in a pluvial-nival watershed, Japan. *J. Am. Water Resour. Assoc*, 44(4): 814-828.

Winsemius HC, Schaefli B, Montanari A, Savenije HHG. 2009. On the calibration of hydrological models in ungauged basins: A framework for integrating hard and soft hydrological information. *WATER RESOURCES RESEARCH*, VOL. 45, W12422. DOI: 10.1029/2009WR007706.

Woodhouse C, Pederson G, Morino K, McAfee S, McCabe G. 2016. Increasing influence of air temperature on upper Colorado River streamflow, *Geophys. Res. Lett.*, 43, 2174-2181. DOI: 10.1002/2015GL067613.

World Meteorological Organization (WMO). 1994. *Guide to Hydrological Practices*, Fifth edition. WMO-No.168.

World Meteorological Organization (WMO). 2012. *Standard Precipitation Index, User Guide*. WMO-No.1090.

APPENDIX A: Information about the Portillo Snowcourse

Snowpack cores are extracted and measured using the “Mount Rose” or Federal Snow Sampling Tube,” as it is a standard to measure SWE (Lopez-Moreno et al., 2020), and it is easy to carry. Depth is measured direct once the sampler is fully inserted into the snowpack. SWE is measured by subtracting the tare weight of the sampler from the SWE plus tare measurement. Snowpack density is computed as the ratio of SWE to depth. Samples are taken along the snow course, normally at locations identify by posts. Depending on the season, samples are extracted every 20 or every 50 meters.

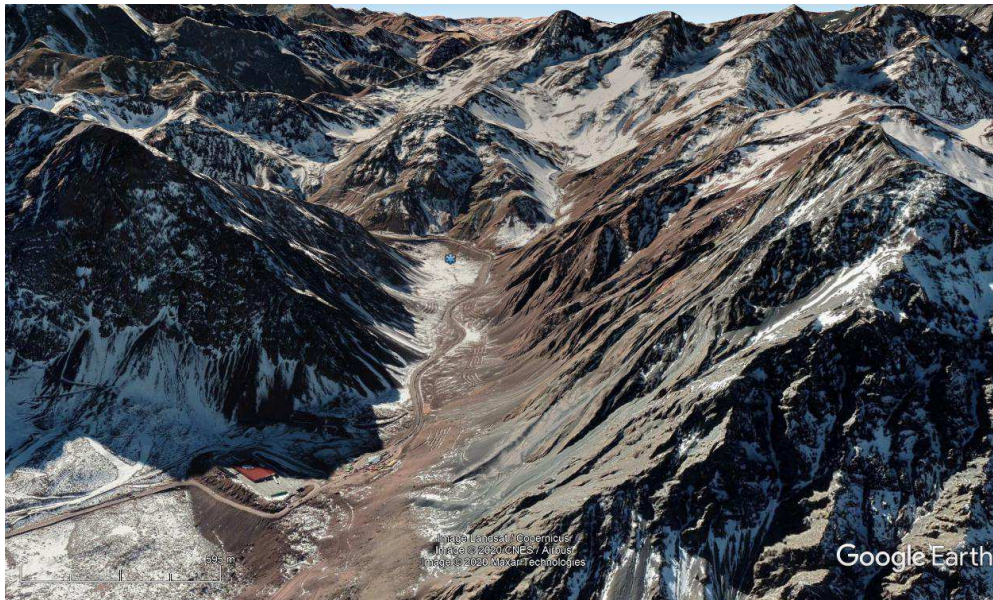


Figure A-1: The snow course (blue point), have its location because availability and logistic are required for these installations. Also, because it was built in 1951, so the resources and transport were limited. From left to right, north to south. Source: Google Earth.



Figure A-2: This picture shows the snow course and its posts. The equipment installed. The conditions of the snow course. From left to right, north to south. Photo from the author Felipe Pérez Peredo.

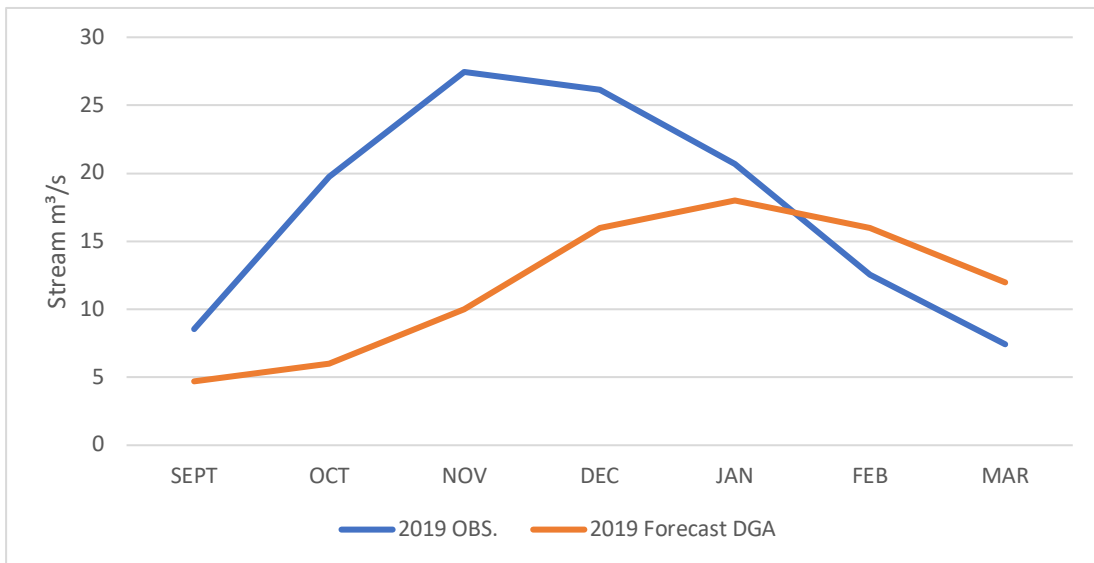


Figure 9-0-1: The figure shows the streamflow for each month in 2019, to the real values and to the forecast made by the DGA.

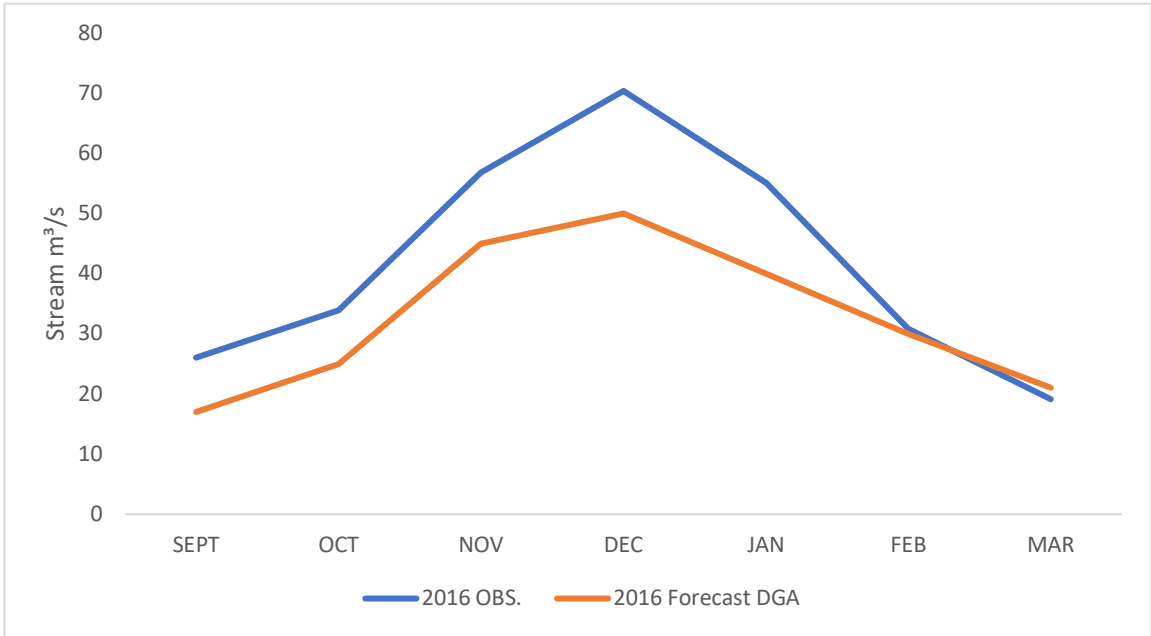


Figure 9-0-2: The figure shows the streamflow for each month in 2016, to the real values and to the forecast made by the DGA.

APPENDIX B: Data used

Table 18: Data used. Volume Estimation.

Year	SWE (mm)	Vilcuya (mm)	Riecillos (mm)	Q August (m ³ /s)	Vol Observed (Hm ³)
1965	261	421	584	26	1103
1966	144	320	458	13	677
1967	47	96	115	7	376
1968	15	45	55	6	244
1969	130	129	251	6	574
1970	487	280	299	11	535
1971	430	132	226	12	608
1972	1208	500	769	25	1782
1973	513	156	295	17	745
1974	1073	284	402	19	876
1975	421	218	315	14	556
1977	1004	382	222	23	1230
1978	1239	372	693	23	1425
1979	400	167	657	14	739
1980	361	311	277	24	1050
1981	1355	214	1091	12	471
1982	1662	617	501	33	1841
1983	597	387	470	20	1142
1984	942	360	248	19	1342
1985	127	144	673	15	667
1986	925	292	1234	22	1298
1987	1521	788	113	50	1800
1988	236	107	452	10	449
1989	640	332	175	15	727
1990	23	119	688	7	407
1991	856	375	541	21	1043
1992	597	457	605	17	876
1993	417	265	293	15	626
1994	526	163	230	15	615
1995	381	183	167	10	483
1996	48	155	914	7	237
1997	1021	700	278	29	1390
1998	690	75	544	11	367
1999	269	246	817	10	641
2000	813	362	282	22	1127
2001	333	301	254	19	920
2002	488	557	835	30	1469
2003	503	200	582	15	669
2004	155	268	329	11	490
2005	1229	472	719	29	1582
2006	775	332	270	22	1073
2007	648	186	165	12	648
2008	546	455	208	24	1073
2009	554	252	302	13	741
2010	320	180	233	9	276
2011	432	173	141	6	315
2012	286	203	302	8	447
2013	322	201	233	8	453
2014	111	169	141	5	312
2015	436	207	263	11	721
2016	460	353	413	18	768
2017	160	255	296	10	404
2018	149	53	131	6	339
2019	10	57	51	5	238
2020	350	202	257	6	390

Q August: Monthly Streamflow August; Vol Observed: Volume controlled at the Station

Table 19: Data used. Monthly Streamflow (m³/s). Rising and falling limb.

Year	January	February	March	April	May	June	July	August	September	October	November	December
1970	41	31	19	11	9	9	9	11	12	23	47	46
1971	32	27	15	10	7	6	10	12	16	30	63	45
1972	36	27	14	10	18	25	21	25	36	41	76	191
1973	179	97	58	28	19	17	19	17	17	24	53	57
1974	65	41	27	17	13	16	20	19	18	40	66	72
1975	73	40	24	15	11	10	11	14	18	24	32	54
1976	40	26	18	14	9	9	8	8	11	17	29	53
1977	44	27	21	12	11	11	18	23	46	58	93	123
1978	74	47	27	17	13	11	25	23	25	45	90	168
1979	125	56	32	19	15	11	11	14	19	29	39	60
1980	63	40	32	37	31	23	22	24	26	39	65	111
1981	70	55	34	19	19	15	11	12	13	20	37	33
1982	34	26	16	14	14	27	40	33	45	51	89	180
1983	167	113	56	29	19	15	18	20	20	52	94	116
1984	75	50	27	17	13	10	17	19	25	67	91	118
1985	101	63	46	24	19	15	16	15	15	21	58	57
1986	45	35	23	16	14	48	25	22	26	42	78	148
1987	101	61	38	19	14	18	40	50	36	55	147	176
1988	150	78	43	24	15	11	9	10	11	18	33	32
1989	31	29	17	11	9	6	7	15	23	39	78	58
1990	36	26	17	11	8	7	7	7	11	19	33	29
1991	25	20	16	12	14	16	27	21	34	38	78	85
1992	80	49	33	19	17	21	18	17	22	41	66	75
1993	65	38	26	20	43	32	16	15	17	28	46	54
1994	44	27	22	14	12	11	12	15	19	25	50	57
1995	40	26	18	13	12	11	11	10	16	18	43	39
1996	26	23	19	12	9	8	7	7	7	9	12	15
1997	19	15	13	9	7	26	22	29	38	40	74	133
1998	146	64	36	26	17	13	12	11	9	17	22	27
1999	25	23	16	10	9	8	9	10	22	37	56	52
2000	37	23	17	13	10	14	23	22	24	56	72	122
2001	78	49	28	16	12	10	13	19	22	43	60	107
2002	57	38	22	14	15	25	26	30	32	51	98	135
2003	127	76	40	20	16	17	17	15	16	33	58	53
2004	45	31	20	14	10	9	9	11	17	16	33	43
2005	34	24	19	11	11	32	20	29	37	54	110	163
2006	135	75	29	16	12	12	28	22	25	47	86	108
2007	81	37	25	14	11	11	13	12	17	31	58	54
2008	42	27	18	13	21	23	14	24	26	45	111	102
2009	61	39	24	16	11	9	11	13	22	28	47	71
2010	53	34	26	15	10	9	9	9	9	12	20	18
2011	17	16	12	8	6	5	6	6	10	16	34	30
2012	25	19	15	10	11	10	10	8	13	15	40	33
2013	32	24	13	8	6	8	8	8	10	18	38	43
2014	31	20	12	9	7	7	6	5	8	19	21	20
2015	21	16	13	8	6	5	6	11	15	20	47	76
2016	58	37	22	22	17	22	18	18	26	34	57	70
2017	55	31	19	17	14	13	12	10	13	18	27	37
2018	23	22	13	10	7	6	6	6	9	11	25	27
2019	24	20	13	8	6	6	7	5	6	6	14	16
2020	20	16	14	7	5	5	6	6	9	20	28	26

Table 20: Data used. Monthly Temperatures (°C). Rising and falling limb.

AÑO	JANUARY	FEBRUARY	MARCH	APRIL	MAY	JUNE	JULY	AUGUST	SEPTEMBER	OCTOBER	NOVEMBER	DECEMBER
1970	17.76	18.82	17.15	15.9	9.72	6.13	9.1	8.2	10.91	11.42	14.43	16.44
1971	17.45	17.64	17.01	13.93	13.36	8.5	11.79	9.64	12.1	16	18.9	19.44
1972	21.69	21.29	18.58	15.59	12.82	10.58	8.81	8.94	11.51	12.69	14.58	19.77
1973	20.93	19.15	17.78	14.62	12.7	8.74	7.99	9.53	11.15	12.67	16.77	18
1974	19.24	18.06	16.69	15.26	10.59	7.4	7.8	12.03	10.45	13.41	16.47	16.97
1975	20.27	18.83	17.31	14.91	12.29	9.86	10.18	8.95	11.15	15.35	17.16	20.97
1977	19.15	18.75	19	15.99	13.71	10.84	7.06	10.75	13.75	12.13	17.34	19.81
1978	20.21	20.31	18.1	17.03	13.94	10.83	14.73	10.96	13.65	15.8	17.3	20.24
1979	19.75	19.65	18.31	15.11	14.27	9.57	11.44	11.69	10.5	14.9	16.39	19.83
1980	21.41	19.78	20.25	15.13	12.6	10.5	10.41	10.84	12.41	14.09	16.84	19.92
1981	20.26	21.3	19.71	16.28	12.54	10.79	10.19	12.51	13.19	14.06	17.45	20
1982	20.77	20.36	18.95	16.05	12.7	9.7	10.54	12.4	12.14	14.42	16.65	20.34
1983	20.57	21.25	19.36	16.52	11.9	7.55	9.16	10.1	10.71	15.77	18.56	20.35
1984	20.92	19.77	18.55	15.79	9.7	7.68	9.28	10.37	12.29	14.2	15.73	18.75
1985	19.63	19.4	17.97	14.27	12.05	12.55	8.9	9.79	12.72	14.36	18.05	19.53
1986	20.95	20.45	19.07	15.03	12.96	10.64	12.24	10.73	11.78	15.63	16.12	20.66
1987	20.48	20.31	19.58	15.33	9.5	11.03	8.76	10.25	11.79	14.6	19.11	20.06
1988	20.64	21.38	18.54	16.23	12.92	10.65	9.31	9.82	10.39	14.73	18.81	20.08
1989	22.16	21.5	18.23	15.5	13.34	11.99	9.69	10.93	11.22	15.09	18.28	20.13
1990	22.07	20.6	18.1	15.09	12.73	12.69	9.76	12.02	12.05	14	15.83	19.72
1991	20.62		19.47	16.15	14.34	12.47	9.21	9.9	13.23	13.52	17.15	17.9
1992	21.52		18.84	14.14	10.73	8.76	9.42	11.57	12.09	15.38	17.08	18.96
1993	20.99	20.5	19.31	14.75	10.9	11.14	9.6	10.91	11.05	14.47	16.68	19.61
1994	20.82	19.76	18.79	16.11	12.62	12.38	10.09	10.75	14.6	14.34	17.86	20.35
1995	20.47	19.45	18.12	16.18	15.36	11.84	7.98	8.89	11.54	14.09	16.65	19.99
1996	19.22	20.07	18.76	13.1	12.44	9.35	11.68	10.51	12.66	14.84	18.5	19.03
1997	20.7	20.77	19.58	16.91	13.12	8.35	10.7	12.03	12.46	12.27	16.35	18.28
1998	21.14	19.56	18	15.01	12.99	11.05	9.67	9.9	11.32	16.26	17.5	19.05
1999	19.35	21.11	17.62	15.26	13.6	10	9.74	10.19	10.49	13.85	16.91	17.47
2000		19.21	18.01	14.65	10.64	7.42	10.13	12.8	10.97	15.97	17.94	
2001	21	21.97	19.5	15.35	12.03	11.04	11.05	11.3	11.17	15.4	16.83	21.31
2002	21.47	21.12	19.42	14.38	13.02	10.6	8.88	11.05	12.55	15.15	17.14	19.35
2003	21.62	20.54	19.8	15.74	13.71	12.12	10.31	12.53	13.64	17.21	19.1	19.75
2004	21.8	20.93	19.46	14.8	11.9	10.63	10.41	11	14.04	14.46	16.68	20.7
2005	21.2	21.19	18.57	15.57	11.54	11.22	9.9	12.1	11.15	14.07	18.13	19.87
2006	22.05	21.41	18.94	16.69	14.45	12.12	11.26	12.03	13.59	14.92	17.49	19.9
2007	21.27	19.66	18.31	15.34	11.26	9.05	8.74	8.07	12.04	14.69	17.63	19.41
2008	21.65	20.88	19.24	15.74	12.93	10.34	9.84	9.92	12.2	14.9	18.6	20.17
2009	21.62	20.69	20.11	18.38	14.23	12.66	9.57	11.38	11.01	15.5	16.02	19.58
2010	21.18	20.22	19.31	16.29	11.93	8.93	7.72	10.46	11.84	14.46	16.66	18.25
2011	20.81	19.79	18.63	14.73	14.16	10.87	8.06	10.41	13.6	14.08	17.27	21.75
2012	21.7	21.51	20.57	14.67	13	10.13	9.34	9.68	12.92	13.07		19.06
2013	21.97	20.89	18.59	15.28	12.14	15.7	9.82	10.28	11.71	15.52		20.85
2014	21.71	19.94	18.24	15.01	11.82	8.75	10.26	12.36	11.76	17.36	17.21	18.72
2015	22.46	21.07	20.18	17.8	13.15	12.1	10.62	11.6	12.36	12.11	16.39	20.3
2016	20.87	22.64	20.46	12.03	12	9.44	9.02	11.42	14.9	14.8		20.05
2017		21.79	19.35	14.8	10.2	9.01	10.34	9.71	11.87	13.6	18.12	20.75
2018	21.27	21.33	18.35	15.2	11	9.76	8.21	10.95	12.16	13.28		